1999-12

Comparison of TAMS/RT surface wind, temperature, and pressure fields with surface observations and model analyses in the socal (sic social) area

Monterrosa, Oscar E.

Monterey, California. Naval Postgraduate School

NAVAL POSTGRADUATE SCHOOL
Monterey, California

THESIS

COMPARISON OF TAMS/RT SURFACE WIND, TEMPERATURE, AND PRESSURE FIELDS WITH SURFACE OBSERVATIONS AND MODEL ANALYSES IN THE SOCAL AREA

by

Oscar E. Monterrosa

December 1999

Thesis Advisor: Wendell A. Nuss

Report Documentation Page	Form Approved OMB No. 0704-0188

1. AGENCY USE ONLY *(Leave blank)*	2. REPORT DATE	3. REPORT TYPE AND DATES COVERED
	December 1999	Master's Thesis

4. TITLE AND SUBTITLE
COMPARISON OF TAMS/RT SURFACE WIND, TEMPERATURE, AND PRESSURE FIELDS WITH SURFACE OBSERVATIONS AND MODEL ANALYSES IN THE SOCAL AREA

5. FUNDING NUMBERS

6. AUTHOR(S)
Oscar E. Monterrosa

7. PERFOMING ORGANIZATION NAME(S) AND ADDRESS(ES)
Naval Postgraduate School
Monterey, CA 93943-5000

8. PERFORMING ORGANIZATION REPORT NUMBER

9. SPONSORING/MONITORING AGENCY NAME(S) AND ADDRESS(ES)

10. SPONSORING/MONITORING AGENCY REPORT NUMBER

11. SUPPLEMENTARY NOTES
The views expressed in this thesis are those of the author and do not reflect the official policy or position of the Department of Defense or the U.S. Government.

12a. DISTRIBUTION/AVAILABILITY STATEMENT
Approved for public release; distribution is unlimited.

12b. DISTRIBUTION CODE

13. ABSTRACT

The Tactical Atmospheric Modeling System/Reat Time (TAMS/RT) combines the high-resolution Coupled Ocean/Atmosphere Atmosphere Mesoscale Prediction System (COAMPS) and the Tactical Environmental Data Server (TEDS).

In this study, we evaluate TAMS/RT sea level pressure, 10 meter (m) winds and 2 m air temperature fields generated at the Naval Pacific Meteorology Oceanography Center (NPMOC) in San Diego. We qualitatively compare outer nest (45 and 54 kms) sea level pressure 12 and 24-hour forecasts with model analyses. Then we quantitatively compare surface observations with inner nest (5 and 6 kms) model wind (u and v) and temperature forecast fields (00, 06, 12, 18, and 24-hour).

Contrary to expectations, we found no error growth through the forecast cycle and relatively high error in the initial analysis for all variables. When examined by 0000Z and 1200Z model runs, we found a repetitive pattern related to the diurnal cycle which impact use by a forecaster. We link day to day error to the diurnal pattern and larger magnitude error to cold starts, background fields, and data assimilation problems. We observed high variability among observed and model values but still found various model trends that require further evaluation.

14. SUBJECT TERMS	15. NUMBER OF PAGES
Mesoscale Modeling, Coupled Ocean-Atmosphere Mesoscale Prediction System (COAMPS), Tactical Atmospheric Modeling System/Real-Time (TAMS-RT), Data Assimilation, Model Verification, Predictability.	82
	16. PRICE CODE

17. SECURITY CLASSIFICATION OF REPORT	18. SECURITY CLASSIFICATION OF THIS PAGE	19. SECURITY CLASSIFICATION OF ABSTRACT	20. LIMITATION OF ABSTRACT
Unclassified	Unclassified	Unclassified	UL

NSN 7540-01-280-5500

Standard Form 298 (Rev 2-89)
Prescribed by ANSI Std. 239-18 298-102

Approved for public release; distribution is unlimited

COMPARISON OF TAMS/RT SURFACE WIND, TEMPERATURE, AND PRESSURE FIELDS WITH SURFACE OBSERVATIONS AND MODEL ANALYSES IN THE SOCAL AREA

Oscar E. Monterrosa
Lieutenant Commander, United States Navy
M.S., University of Puerto Rico, Mayaguez, P.R., 1986
B.S., University of California, Santa Cruz, 1982

Submitted in partial fulfillment of the
requirements for the degree of

MASTER OF SCIENCE IN METEOROLOGY AND PHYSICAL OCEANOGRAPHY

from the

NAVAL POSTGRADUATE SCHOOL
December 1999

Author: [redacted]
Oscar E. Monterrosa

Approved by: [redacted]
Wendell A. Nuss, Thesis Advisor

[redacted]
Douglas K. Miller, Second Reader

[redacted]
Robert L. Haney, Chairman
Department of Meteorology

ABSTRACT

The Tactical Atmospheric Modeling System/Real Time (TAMS/RT) combines the high-resolution Coupled Ocean/Atmosphere Mesoscale Prediction System (COAMPS) and the Tactical Environmental Data Server (TEDS).

In this study, we evaluate TAMS/RT sea level pressure, 10 meter (m) winds and 2 m air temperature fields generated at the Naval Pacific Meteorology Oceanography Center (NPMOC) in San Diego. We qualitatively compare outer nest (45 and 54 km) sea level pressure 12 and 24-hour forecasts with model analyses. Then we quantitatively compare surface observations with inner nest (5 and 6 km) model wind (u and v) and temperature forecast fields (00, 06, 12, 18, and 24-hour).

Contrary to expectations, we found no error growth through the forecast cycle and relatively high error in the initial analysis for all variables. When examined by 0000Z and 1200Z model runs, we found a repetitive pattern related to the diurnal cycle which impact use by a forecaster. We link day to day error to the diurnal pattern and larger magnitude error to cold starts, background fields, and data assimilation problems. We observed high variability among observed and model values but still found various model trends that require further evaluation.

TABLE OF CONTENTS

ACKNOWLEDGEMENTS

Many thanks to Dr. Wendell Nuss, Assistant Professor, Department of Meteorology, Naval Postgraduate School, for his guidance and insight. From programming to mesoscale meteorology, his help was invaluable. Drs. Doug Miller, Chuck Wash and Tom Herbers also provide valuable insight and assistance.

Also, muchas gracias to CAPT Chris Gunderson for instigating my thesis development and proving the adage that "you can run, but you can't hide." Thanks to the crew at the Naval Pacific Meteorology and Oceanography Center in San Diego for providing the TAMS/RT fields.

Ms. Mary Jordan, Mr. Dick Lind, Mr. Bob Creasey, and Mr. Mike Cook of the Departments of Meteorology and Oceanography, Naval Postgraduate School, all gave unselfish and critical assistance throughout the analysis of the data.

My amigo A.J. Reiss helped at various stages throughout the process. Lastly and most importantly, merci beaucoup Isabelle for overall loving support and editing (the support was loving, however the editing was ruthless...). My wonderful kids Kristelle and Gabriel, and my grandmother, Carmen, kept me in check as to what's really important in life, gracias, besitos...

I. INTRODUCTION

A. WHAT IS SO SPECIAL ABOUT MESOSCALE MODELS?

The United States Naval Service maintains roles of deterrence, sea superiority, and the protection of maritime trade. However, in the past decade its focus has shifted from a global to regional emphasis highlighting littoral operations (NDP 1, 1994). Recent technological improvements in mesoscale numerical weather models have increased the Navy's interest in detailed, short-term forecasting (Hodur 1997). High-resolution topography and Graphical User Interface (GUI) displays provide a four-dimensional view of the surface and atmosphere, including depictions of jet streams, vertical motion, and moisture. Researchers are able to initialize mesoscale models with local and particular observations, and to experiment with specific analysis and/or model physics schemes unavailable to operational centers (Miller 1999). Meanwhile, forecasters are drawn to mesoscale models due to their ability to focus on areas of interest with higher resolutions. Mesoscale models capture many details of mesoscale phenomena (Doyle 1997, Warner 1992, Thompson et al 1997), nonetheless, questions remain about mesoscale model accuracy and their most appropriate use for forecast guidance.

B. FORECASTER GUIDANCE USING MESOSCALE MODELS

Forecasters need to understand model characteristics. When using a global model, a forecaster typically evaluates the model analysis with local observations, satellite images, and forecasts from another model or previous model run to determine how well a model is "handling" the synoptic situation. Then he/she takes the model forecast and applies rules of thumb about local topography and known model tendencies to produce a forecast. A forecaster's skill is measured by how well he/she applies these local rules to recurring situations and how well he/she knows when not to believe the model output.

Can this same procedure be applied when using mesoscale models is a central issue motivating this study.

C. PREDICTABILITY

Predictability theory states that atmospheric predictability varies with time, seasons, geographic location, and synoptic pattern with error growing over time. Moreover, smaller scales of atmospheric motion are forecast with less skill than larger scales due to inherent differences in the predictability error growth for different scales of motion (Anthes 1986). High-resolution alpha and beta mesoscale models (2 to 200 kilometers) imply "high-variability" within their domain (at least compared to global models). Variability increases under weak synoptic forcing. Typically, improving a forecast means reducing model error for all variables (wind, temperature, precipitation, etc.) throughout the entire domain. At present, it may be unrealistic to expect a high-resolution model to improve all variables, all the time, everywhere within the domain, especially under weak synoptic forcing. Model accuracy can be improved by reducing model error. Any attempt to improve the model forecast must explore the nature of model error. As a start, we should attempt to verify and to understand a model's tendencies by learning how error for variables of interest varies over time and space.

C. MODEL VERIFICATION

Numerical models can be compared with a model-generated analysis or, with observations. When comparing mesoscale models with observations, the largest and most difficult verification problem is with the lack of mesoscale observations (Perkey 1986). In theory, observational data should be the most accurate picture of the atmosphere but could also lead to local effects not representative of a larger area. Also, the verification is biased towards areas where observations are available. On the other hand, verification of a model forecast with a model analysis is only as good as the model analysis. The

Cooperative Program for Operational Meteorology, Education and Training (COMET) Module provides an excellent description of the advantages and disadvantages of each scheme (COMET Numerical Prediction Module 1998).

D. OBJECTIVES

In this study, we use both verification methods to evaluate sea level pressure, 10 meter (m) winds and 2 m air temperature fields generated by the Tactical Atmospheric Modeling System/Real Time (TAMS/RT) located at the Naval Pacific Meteorology Oceanography Center (NPMOC) in San Diego. We examine error growth through the forecast cycle and relate it to predictability theory. In addition we look for model trends and characteristics.

THIS PAGE INTENTIONALLY LEFT BLANK

II. MODEL DESCRIPTION

The Naval Research Laboratory's (NRL) TAMS/RT processes the atmospheric component of the Coupled Ocean/Atmosphere Mesoscale Prediction System (COAMPS). COAMPS is a triple-nested non-hydrostatic mesoscale model using a multi-variate optimum interpolation (MVOI) data interpolation scheme. Features include a globally relocatable grid, user-defined grid resolutions and dimensions, nested grids, an option for idealized or real-time simulations, and code which allows for portability between mainframes and workstations. It derives its initial and lateral boundary condition fields from the Navy Operational Global Atmospheric Prediction System (NOGAPS) run at Fleet Numerical Meteorology and Oceanography Center (FNMOC). When the model is initialized directly from a NOGAPS analysis or forecast, the process is called a "cold start" (Hodur 1997).

TAMS/RT also includes the Tactical Environmental Data Server (TEDS). TEDS allows independent ingest of local observations and satellite-derived observations and boundary conditions from a central or regional center and maintains an on-site data assimilation, nowcast, and forecast capability. A unique feature of TAMS/RT compared with other mesoscale modeling systems is the ability to operate in data assimilation mode - feeding observations into the COAMPS forecast cycle. In the mesoscale data assimilation scheme, the previous model forecast is used as a starting point and the observed data is incorporated in order to initialize the next model forecast. This process or, "warm start," is repeated every 12 hours and, although not verified, is considered the ideal method of initializing a model run. The TAMS/RT nowcast is when this cycle is used to regularly update just the local model forecast field using the analysis (without a subsequent forecast). This nowcast feature is designed to automatically maintain a database containing the best estimate of the current environmental conditions within the domain (TAMS/RT homepage, 1999).

Reiss (1999) provides an excellent summary of NPMOC's TAMS/RT system characteristics and specific configurations (Table I).

THIS PAGE INTENTIONALLY LEFT BLANK

III. METHODS

A. TECHNIQUE

From 22 March to 22 September 1999, we analyzed inner nest 5 and 6 kilometer (km) wind and temperature analyses and forecast grid fields. Outer nest 45 and 54 km sea level pressure fields were examined from 11 May to 22 September 1999. NPMOC defined the outer, middle, and inner nests as 45, 15, and 5 kms before 18 June, and 54, 18, and 6 kms afterwards (Fig. 1).

Both 0000 UTC and 1200 UTC (hereafter 00z and 12z) model run analysis and forecast grid files were transferred via file transfer protocol (ftp) daily to the Naval Postgraduate School (NPS) with back-up 4mm magnetic tapes sent to NPS bimonthly. Surface and ship observations are continuously received and archived at NPS.

VISUAL, a FORTRAN-coded diagnostic and display program (Nuss and Drake 1995), was used to plot sea level pressure fields for outer and middle nests for 12 and 24-hour forecasts. Additionally, VISUAL was used to plot and compare surface observations with model wind and temperature fields for the inner nest for analysis, 6, 12, 18, and 24-hour forecasts (hereafter referred as f00, f06, f12, f18, f24, respectively). These computed differences were saved for subsequent statistical analysis. In all cases both 00z and 12z model runs were examined.

FORTRAN and MATLAB programs were used to sort and file data, compute statistics, and create time series plots. Microsoft EXCEL was used to create spreadsheets and scatter plots for monthly and station analysis. Other information used to compare with VISUAL plots includes high-resolution (4 km) satellite imagery and NPMOC and National Weather Service forecast discussions.

B. TERMINOLOGY

To avoid confusion, model runs will be referred to as 00z or 12z while valid times will be listed as either 0000, 0600, 1200, or 1800 UTC. Throughout this report we refer to specific forecasts of a certain model run using the following notation:

29/12z f18 = 29 (day) / 12z (model run) f18 (18-hour forecast)
00z f00 = 00z model run, analysis
12z f06 = 12z model run, 6-hour forecast
00z f24 = 00z model run, 24-hour forecast, and so on.

C. SEA LEVEL PRESSURE COMPARISON

To qualitatively assess if mesoscale error fluctuations corresponded to synoptic-scale error, 12 and 24 hour forecast sea level pressure fields were compared with the verifying model analysis. These plots were generated for both 00z and 12z model runs, for both outer and middle nests.

San Diego and the Southern California (SOCAL) bight were used as benchmarks to determine forecast fit for the outer domain. Isobars at 2 millibar (mb) intervals were examined and the difference between model and analysis isobars was measured in the SOCAL area. 00z and 12z model runs at 12 and 24-hour forecasts were compared for "best fit" or lowest pressure difference between forecast and analysis. In addition, the tendency for the model to have either higher or lower pressure compared to the analysis was recorded.

D. WIND AND TEMPERATURE COMPARISONS: OBSERVATION - MODEL = ERROR

East/west (u) and north/south (v) wind vectors at 10 meter height, and 2 meter air temperature variables were compared by subtracting model from

corresponding observed values (observation - model = error). A two-dimensional multi-quadratic interpolation scheme was used to interpolate grid points to observations (Nuss and Titley 1994). VISUAL plots show wind and air temperature fields along with error values for temperature and wind speed and direction error vectors for each reporting station (Fig. 2). Below is an example of wind vector and station error notation on VISUAL plots:

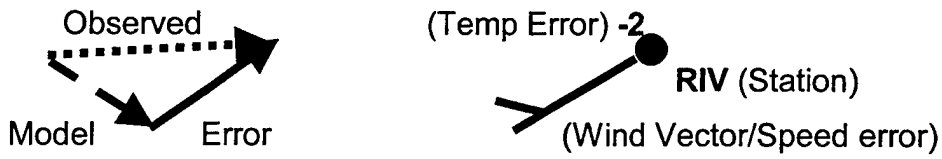

Approximately 40 surface reporting stations are within the inner nest domain with 8 to approximately 36 stations reporting at any given forecast validation time. Ship reports were received sporadically and incorporated into the data set. Figure 3 shows the 5 km nest SOCAL topography with a sample of some reporting stations.

E. DATA ASSIMILATION

Data assimilation information was gathered for most of August and September and retrieved from NRL's TAMS/RT web page (NRL TAMS/RT web page). In assessing the impact on error growth we designated two categories of data assimilation. Full data assimilation included: rawinsonde observations (raobs), surface observations, satellite winds, pibals, Special Sensor Microwave/Imager (SSM/I) winds, aircraft reports, and NOGAPS generated rawinsonde observations (pseudo-raobs). Limited data assimilation included the same data as full, except for raobs and surface observations.

F. TIME SERIES PLOTS

Time series plots of daily averages of u, v, and temperature were

generated for selected forecasts (f00, f06, f12, f18, and f24) and time periods (by season and by month). The purpose of the time series was to show error variability over time and outline periods when errors were greatest in order to examine possible relationships and sources of error.

IV. RESULTS

A. SYNOPTIC PATTERN

In April, several low pressure systems moved across California and the Pacific Northwest. For most of May to September a summertime synoptic pattern dominated. This pattern consists of a strong semi-permanent East Pacific high pressure system that interacts with a low pressure trough extending north from Mexico across California (NPMOC Forecasters Handbook). The resulting pressure gradient was typically west to east along the West Coast.

Throughout the sampling period, local and remote data ingest into TEDS varied considerably as did the TAMS/RT initialization routine (warm versus cold start). Due to a TEDS malfunction, there was a documented period of very limited data assimilation (NOGAPS pseudo-raobs only) and frequent cold starts (2-3 times per week) from 7 to 20 April.

Seasonal analysis varied from 22 March to 17 June (spring), and 18 June to 22 September (summer). We chose 18, rather than 22 June since it corresponded with NPMOC's shift from a 5 to 6 km inner nest grid (on 00z model run).

B. SEA LEVEL PRESSURE COMPARISON

Throughout the study period, the outer nest sea level pressure forecasts performed remarkably well. For the most part, major features were captured and isobars, especially over water, paralleled and closely followed the analyses.

Figure 4 is an example of analysis and verifying 12 and 24-hour forecast of TAMS/RT sea level pressure for the outer nest (54 km resolution). Using the SOCAL area as a benchmark, this example for the 00z model run on 28 August shows that both forecasts capture the major synoptic features, however, f24 does a better job with the central pressure of the thermal low over southwestern Arizona. In the 28/00z f12, analysis sea level pressure over the San Diego area is approximately 1012-13 millibars (mb) while forecast pressure is 1010-11 mb.

Meanwhile, the 28/00z f24 analysis shows 1012 mb while the forecast has 1010-11 mb. Other criteria to assess best fit include the distance between forecast and analysis isobars. In Figure 4, the distance between the 1012 mb isobars over the San Diego area is approximately 65 nautical miles (nm) for the f12 and less than 40 nm for the f24. In this case, the f24 has a better fit for outer nest sea level pressures in the SOCAL area.

Similar observations were noted from May to September along with the percentage of times that f12 (or f24) gave a better pressure forecast than f24 (or f12). Table II outlines these results including a qualitative assessment of best fit between model forecast and verifying analysis.

Clearly, the 12z f12 gave the best SOCAL sea level pressure forecast (94% better fit than f24) followed by the 00z f24 (65% better fit than f12). Both these forecasts were valid at 0000 UTC or 1700 local, corresponding to the warm portion of the diurnal cycle when surface pressures are expected to lower over land. On the other hand, the 00z f12 and 12z f24 consistently gave a worse fit, with 1-4 mb lower sea level pressures 95% of the time. Both these forecasts were valid at 1200 UTC or 0500 local and correspond to the cold part of the diurnal cycle when pressures over land increase. For the cases where the model forecasted equal or higher pressures, values ranged from 0-2 mb.

These results suggest that TAMS/RT is not resolving diurnal effects. Using Figure 4 as an example, the 28/00z f24 is valid at 0000 UTC (warm cycle) and shows good agreement between forecast and analysis with placement and central pressure for the Arizona thermal low. At night, the thermal low fills slightly and the 00z f24 valid 1200 UTC (cold cycle) shows that the forecast has pushed the trough too far to the west and has the central pressure 2 mb lower than the analysis. This is most likely due to coarse model resolution, especially of the coastal topography. Thus, the model does not "feel" the coast and pushes the trough offshore resulting in a tighter west/east pressure gradient that is offset from the analysis.

C. SEASONAL COMPARISON

Figures 5a, b, c, d, depict analysis (f00) and forecast (f24) time series plots for spring and summer for both (00z and 12z) model runs. They show

mean daily bias averaged from all the stations that reported within the inner nest for that verifying time, along with corresponding standard deviation and Root Mean Square (RMS) error.

April, June and August had distinct periods of high temperature error while high wind error occurred in April, nearly concurrent with the period of increased temperature error (Figs. 5a, b, c, d). Specifically, high positive u error, increased variability in v error, and high negative temperature error occurred between 10 to 20 April in the analysis and persisted throughout the forecast cycle. In June, high negative temperature error is evident on the 14 June analysis (f00) with no noticeable change in wind error and again, persisted throughout the forecast. The third noticeable instance of high negative temperature error occurred between 27 and 30 August with no apparent change in wind error. This high negative error did not appear in the forecast. These three cases will be examined more closely later.

Figure 6 shows that there was no error growth in the forecast cycle for u, v or T, in either spring or summer. This finding contradicts our expectation from predictability theory that error starts small and will grow during the forecast cycle (Anthes and Baumhefner 1986). We found that error starts high and both error and variability remain high throughout the forecast.

Temperature and north/south (v) wind error was larger in spring than in summer, probably due to stronger synoptic forcing in spring. East/west error was larger in summer due to a more prevalent sea/land breeze circulation. A positive bias for all variables for all forecasts (recalling that observations – model = error), indicates that overall, TAMS/RT underforecast wind speed and temperature in both spring and summer months. However the large variability shown by the error bars for v and T (u is not shown but is of similar magnitude) and high RMS indicates that there were many variations (Fig. 6). Highest temperature errors in spring and summer occurred at f06 and f18 and again hint at a model problem with resolving the diurnal cycle since part of these forecasts (depending on model run) are valid at 1800 UTC (warm cycle).

V error also peaked at f06 and f18 implying there may be a similar link to the diurnal cycle. All variables reflect relatively large daily variability that is most likely due to topographical flow and differential heating of land and sea within the domain.

Figure 6 also shows that the occurrence of minimum error is different for v than for u and T. This is probably a reflection of seasonal change between greater synoptic forcing in spring when more major frontal systems are influencing the area, and less in summer when there is a weaker north/south component and a steady west/east pressure gradient.

D. MODEL RUN COMPARISON

The spring and summer error distribution observed in Figure 6 led us to think there might be a relationship between error growth/decay and the diurnal cycle. We examined the averages of monthly error averages from 1 April to 22 September for each forecast of each model run (00z and 12z). The result, (Fig. 7), clearly shows a different trend than that observed with combined model runs in Fig 6.

All three variables followed a distinctive pattern of error growth/decay that repeats itself 12 hours later in the following model run. Between the maximum and minimum values, u, v, and T profiles for both model runs follow nearly identical paths. Highest errors for u and T occurred during the warm portion of the diurnal cycle when westerly winds predominate and temperatures are at their maximum.

Temperature had the largest errors with maximum values of 3.2 to 3.4 degrees Centigrade (°C) occurring at 1800 UTC, or 1100 local (verifying forecast: 00z f18 and 12z f06). When these errors are compared to average observed temperature, they account for about 16% of the observed mean value (Fig. 7). Minimum temperature errors were at 1200 UTC, or 0500 local (00z f12 and 12z f00) when temperatures are lowest and are about 4% of the observed mean.

East/west or u error followed a similar error pattern with maximum error of 0.8 to 1.0 meters per second (m/s) at 1800 UTC (00z f18 and 12z f06) that provides 48-52% of the observed mean value. Minimum values of 0.25 to 0.35 m/s, occurred at 0600 UTC, or 2300 local (00z f06 and 12z f18) and account for 16-21% of observed mean value.

The north/south or v wind component had the smallest errors and followed a similar but less obvious pattern. The range between error values was 0.2 to 0.6 m/s with a maximum at 1800 UTC (00z f18 and 12z f06) and corresponded

to 70-76% of the observed mean value. Minimum v error of 0.19 and 0.22 m/s occurred at 0000 UTC (00z f24 and 12z f12) and accounts for 24-28% of the observed mean value.

Overall, the resulting pattern is all errors decreased as temperatures cooled and increased with warming. A possible explanation for this trend and its relationship to model topography will be discussed in the next chapter.

E. INITIAL ERROR

Table III compares RMS error and initial bias (f00) to the corresponding observed u, v, and T average observed values. For u and v, the bias is not really wind speed dependent while the temperature bias is temperature dependent.

Figure 7 gives the impression that the inner nest 12z analysis (f00) values are low, Table III shows that relative bias at time of initialization is high for both model runs, especially the 12z model run. In addition, the large u and v RMS error show that the magnitude of the absolute error is very high for the analyses of both model runs.

F. AVERAGE WIND ERROR

In a southern California summer regime, winds offshore are typically northwesterly. During the day, they become more southwesterly along the coast and a steep coastal thermal gradient creates a strong onshore sea breeze (NPMOC Forecasters Handbook, 1995). Further inland, complex topography modifies the wind flow.

Table IV outlines observed and model average wind vector (u, v) direction along with combined average wind direction and speed for all stations. At all times and for both model runs, the model underforecast the predominant westerly wind component. For the north/south component, the model underforecast the stronger daytime southerly flow and overforecast the light, nighttime northerly flow. This pattern further demonstrates the diurnal character of the wind flow.

G. VARIABILITY

It is important to note that there is high variability behind these results. Although variability is low among the monthly averages in Figure 7 (error bars are not displayed), there is a large amount of variability in the data used to compute each monthly average (monthly values range from 2-3 m/s and 2-4 °C).

Figure 8 shows that model variability is in the same range as the observed variability, however there are some significant differences. During the warmest part of the day (1800 and 0000 UTC), the model displays less variability than the observed atmosphere. At the coolest part of the night (1200 UTC), the opposite occurs and the model has more variation than observed for both temperature and wind. In this case, the model's lack of diurnal forcing and smoother-than-real topography allows greater variation in the wind flow than the actual topography permits, especially over inland areas.

H. MODEL TOPOGRAPHY VERSUS ACTUAL

The variability differences between model and observed values may result from model topography that is smoother than real. Figure 3 shows model topography for the inner nest and Table V is a comparison of model and actual elevation for some of the inland stations within the inner nest. Using a 6.5 °C per 1 km lapse rate, the difference between model temperature and actual may range from 3 to 5 °C. This would account for the consistent temperature bias shown for the analysis in Table III at 00z but does not fit the lower temperature bias at 12z. The tendency for a cold model bias inland would generally result in a weaker sea breeze and low wind variation during the warm times.

I. RECAPITULATION

So far, we have demonstrated the following:

- Error in the initial conditions is not reflective of forecast error.
- The pattern of error growth and decay is a reflection of the model producing a weak warming and cooling cycle over land (low amplitude).
- The model does not capture all the daytime variability in wind and

temperature nor does it accurately follow the diurnal cycle and that this is probably related to differences between the model and actual topography.

At this point, we would like to present some specific examples that will give further insight into the nature of the relationship of the diurnal cycle and observed error pattern.

THIS PAGE INTENTIONALLY LEFT BLANK

V. CASE STUDIES

A. SYNOPTIC INFLUENCE ON MESOSCALE FORECAST

The general consensus among forecasters is that synoptic error is correlated to mesoscale error (Gunderson 1998). A good synoptic fit should lead to a good mesoscale forecast. We present three outer nest examples of model runs with a good synoptic scale sea level pressure fit for which the corresponding mesoscale forecast showed large errors, especially with temperature. If we assume that synoptic scale temperature is also well fit, then the high error displayed in April, June, and August (Fig. 5) contradict the notion that a good synoptic fit implies a good mesoscale analysis and forecast.

On 11 and 12 April a low pressure system moved across SOCAL. Figure 9 depicts the outer nest 11 April 00z f12 and verifying 12z model run analysis. Although central pressures for both the depression located over northern California and the ridge over SOCAL are off by 2 mb, it appears that the model had a relatively good handle of synoptic features and sea level pressure distribution. The VISUAL plots of the inner nest (Figs. 10 and 11) show high temperature errors of 1 to 8 °C inland, and 0 to 4 °C along the coast (11/00z f12 and 11/12z f00). Six hours, later both 11/00z f18 and 11/12z f06 show even higher temperature errors (6 to 11°C inland and 1 to 5 °C along the coast) along with wind speed and direction errors, namely over the interior regions. For this case, high error was probably related to frequent cold starts, strong synoptic forcing and very limited data assimilation.

Figure 12 shows that the 13 June 12z f12 valid on 14/00z verified very well with the analysis. On 14 June, Figure 5 shows that there was a large negative temperature error for both model runs that persisted through the forecast.

Finally, Figure 4 shows the 28 August 00z analysis, f12 and f24. Both forecasts capture major synoptic features although the f24 does a better job with central pressures. Again, Figure 5 shows that high temperature errors occurred during this period.

Assuming synoptic scale pressure is positively correlated to synoptic scale temperature, these examples show that:

- *Good synoptic fit does not ensure a good mesoscale forecast.*

Most of the synoptic scale cases observed during this study verified remarkably well and gave little to no indication of the magnitude of mesoscale error.

B. APRIL

April shows the effects of cold starts, warm starts with very limited data assimilation, and the possible effects of lateral boundary conditions on the inner nest. Considerable synoptic scale activity dominated the month. Various low pressure systems moved across the central and northwest coast of the United States, some of which influenced the SOCAL region. Figure 5a shows that high u, v, and temperature errors occurred from about 10 to 30 April. During that time, there was a period of very limited data ingest (NOGAPS pseudo-raobs only) into TAMS/RT due to a TEDS malfunction that lasted from 7 to 20 April. As a result, NRL recommended that NPMOC cold start the TAMS/RT 2 to 3 times per week.

Figure 10 shows 11 April 00z f12 and f18 VISUAL plots while Figure 11 portrays 11 April 12z f00 and f06 plots. Figure 10 plots are valid at the same time as Figure 11. With a warm start and very limited data assimilation, it is not surprising that the 00z f12 and 12z f00 are identical. Shown also, are the 00z f18 and 12z f06, valid six hours later. Over land, the wind and temperature fields are very similar and continue to have high errors. This shows a comparable handling by the model of surface heating and topography. Offshore, wind flow has changed notably from southwesterly to southerly in the southwest corner of the inner nest (around San Clemente Island). This difference is probably due to one or more of the following: the influence of NOGAPS pseudo-raobs which may introduce a NOGAPS bias such as warm inland temperatures into the model run (Nuss pers.comm.), the influence of lateral boundary conditions (updated every 12 hours) that could possibly contaminate the forecast especially with a rapidly evolving synoptic situation such as in this case (Sashegyi and Madala 1992), or, the difference in adjustment time of the model from its initialization. Although

inconclusive as to which depiction of offshore flow is better, the Santa Catalina buoy (4602) indicates that the 00z f18 forecast captured the wind direction at that location better than the 12z f06. This example points out that:

- *The effect of lateral boundary conditions and NOGAPS pseudo-raobs on error growth needs to be investigated.*
- *Major adjustments in offshore wind flow can have little impact on coastal and inland temperature and wind fields.*

C. AUGUST AND SEPTEMBER

August and September are examples of the effects of cold and warm starts including both detrimental and possibly beneficial aspects of data assimilation.

In early August there were frequent TAMS/RT system crashes along with a NPS server problem. Figures 13 and 14 are time series for August and September analyses (f00) for both model runs with days of full and limited data ingest highlighted (see Methods section for a definition of "full" and "limited" data ingest).

There is more variability in temperature error for both model runs in August than in September. Initial (f00) error distribution in September follows the average trend (Fig. 7) of higher error at 00z than 12z. In August, 00z mean error or bias followed the average trend of colder temperatures than observed, but the overall bias for the 12z model run was actually negative indicating that on average the model temperature was too warm. Closer examination of Figure 14 indicates that two peaks (16 and 26-31 August) skew the bias negatively.

1. 16 August Episode

The negative temperature error peak on 16 August was most likely caused by a poor background field following a cold start after a system crash of the previous 16 August 00z model run. Figure 15 shows that on 16 August, the 12z f00 analysis had a smoothed temperature field with light offshore flow and high wind and temperature errors throughout the domain. Six hours later, the model developed a more realistic temperature and wind flow pattern; errors were lower and temperature was again too cold but in accordance with the average

trend (Fig. 7). The 12z model run initialized with limited data assimilation (no surface observations or raobs) and either a NOGAPS 12-hour forecast or the previous TAMS/RT 24-hour forecast, whichever the case, it forced the initialization to be too warm. Figure 16 shows the 12-hour forecast and corresponding analysis from the following model run. Only limited data assimilation took place. Clearly, the 16/12z f12 and 17/00z f00 wind and temperature fields are identical. This example shows the following:

- *A cold start can introduce large errors into the analysis through the background field.*
- *Six hours after a cold start with a poor background field, the model has developed a more realistic wind and temperature field.* Model physics along with the diurnally cycle maintains the error pattern previously described.
- *In a warm start, errors present in the background field or 12-hour forecast are carried into the next model run.* Those errors follow a repetitive pattern related to the diurnal cycle that repeats itself every 24 hours.
- *With limited data assimilation, the model quickly recovered and within one model run of the high error episode, was back to the norm observed in Figure 7.*

2. 26 August Episode

Between 26 to 30 August, 00z and 12z model runs displayed a broad negative temperature peak. Previously, both 26/12z and 27/00z model runs had crashed and either the background field and/or the full data assimilation scheme that occurred during this time, introduced high negative temperature errors into the 27/12z model run. Contrary to the 16 August case, this negative bias actually got worse before gradually returning to the norm by 31/00z. This is an example of data assimilation leading to increased analysis errors.

Figure 2 shows how the model, by 12 hours, has developed a realistic depiction of the thermal gradient and wind flow (27/12z f12). However, when used as a background field to warm start the following model run with full data assimilation, the analysis (28/00z f00) has lost the high temperature resolution and both wind and temperature errors are high throughout the domain. A warm

start initiated this model run and therefore the only explanation is NOGAPS-smoothing (from pseudo-raobs) that has destroyed any detailed mesoscale structure.

This pattern of high- resolution 12-hour forecasts leading to low – resolution analyses due to poor data assimilation at initialization (warm start) continued through 6 model runs.

Effects of poor initialization are further highlighted in time series of forecasts for individual stations. Figures 17a and 17b are time series for inner nest model and observed u, v, and T, for 28/12z and 29/00z model runs for both North Island (San Diego) and Riverside (inland valley). Notice the differences between the 28/12z f12 and 29/00z f00 values. At North Island, u remains the same, v improves, and T worsens. At Riverside, u, v, and T all worsen. These differences in the analysis are presumably due to data assimilation. Comparing 28/12z f24 and 29/00z f12, North Island u and T improved while v worsened, meanwhile at Riverside all variables improved. This pattern of reduced forecast errors for Riverside (u, v, and T) after full data assimilation and high analysis errors, warrants further investigation.

- *Data assimilation (or the assimilation of unrepresentative data) can increase the time it takes for the model to recover from high initial errors (i.e., return to mean levels).* If the data introduced into the initialization smooths the analysis, then it will take longer for model physics and diurnal tendencies to restore a high level of structure to the forecast.
- *In a warm start, large-scale data assimilation (i.e., from the global model) can smooth out any fine scale thermal structure that was present in the background field.* Any fine detail observations will probably be lost from the effects of the large-scale circulation analyzed aloft (Hovermale 1986).
- *Data assimilation can affect u, v, and T differently at different locations within the domain.* Data assimilation can be weighted towards improving certain variables in certain locations under certain circumstances. The example with North Island and Riverside highlights the complexities of mesoscale forecasting and analysis.

3. September

September may be an example of a beneficial data assimilation procedure. Figure 14 shows that during most of September full data assimilation took place. On the two documented occasions (2-3 and 9 September) of limited data assimilation, the temperature bias increased. Regardless, even with full data assimilation, the monthly bias was in agreement with overall average temperature bias for the entire study period (Fig. 7).

Interestingly, after a series of system crashes on 18-19 September, the following model run initialized using full data assimilation and had an average daily error only slightly above the monthly bias.

- *Data assimilation with surface and rawinsonde observations (i.e., full data assimilation) may produce lower initial errors than without (i.e., limited data assimilation).*

4. Inland/Coastal Comparison

To assess which region, inland or coastal, contributed higher errors in August, we examined temperature time series (analysis) for stations in the San Diego area and inland regions (Fig. 18). San Diego stations display similar biases as that observed during August for all stations (Fig. 13) with little variation between the 5 to 7 reporting stations. Meanwhile, inland stations have much larger positive (00z) and negative (12z) bias and larger variation (9 to 11 stations reporting) that is reflected in both model runs.

- *Under weak synoptic forcing and terrestrial heating, inland areas contribute the largest errors within the domain.*

D. RIVERSIDE

To show the impact of topography on temperature error we plotted the spring and summer temperature error distribution for Riverside for both model runs (Fig. 19). Riverside is located on an elevated plateau between the Santa Ana and San Bernardino mountains, approximately 35 nm from the coast.

Error trends in the Riverside forecast cycle are similar to all stations averaged (Fig. 7). The range of error is higher at Riverside in both spring and summer. Spring temperature bias is too cold throughout the forecast. In

summer however, the model has a cold bias at all times except 1200 UTC, when model temperatures are consistently too warm.

As shown previously (Table V), model elevation at Riverside is too high making model temperature values too cold. Attempting to reduce the cold bias by correcting for elevation (623 meter difference) produces approximately 3 °C difference. Using Figure 19, applying a 3 °C correction improves the temperature forecast during the day. However, applying the same correction at night actually makes the error worse since the model now has a warm bias.

- *The model is poorly capturing the diurnal cycle over inland areas; it is too cold during the day and too warm at night.*
- *For inland areas, correcting for elevation improves a daytime temperature forecast but worsens a nighttime one.*

E. AVERAGE TRENDS: 22 MARCH TO 22 SEPTEMBER 1999

The following is a collection of the average trends observed during this study:

1. Synoptic scale forecasts (outer nest) valid during the warm cycle (0000 UTC) give the best sea level pressure forecasts. This is when the model has the best handle on placement and central pressure of the thermal low.
2. Synoptic scale forecasts (outer nest) valid during the cold cycle (1200 UTC) underforecast sea level pressures. The coarse resolution of the model's outer domain does not allow it to differentiate the coastline and pushes the thermal trough too far west.
3. Inner nest bias is greatest during the warm cycle, lowest during the cold cycle.
4. Inner nest bias is greater over inland areas in summer.
5. The model has a cold bias throughout the inner nest with the following exception noted below.
6. In summer, differences between real and model terrain height compound the temperature problem in that the model is too cold during the day and too warm at night in the inland region. This in turn might impact the diurnal cycle.
7. Inner nest initial and forecast wind errors for either model run are relatively high when compared to average observed wind. Error contribution varies from 20 to over 200%.

8. Inner nest TAMS/RT average forecast east/west (u) wind values are consistently lower than observed. Inaccurate model topography is most likely the cause.
9. The north/south (v) wind component is underforecasted when winds are from the south (daytime) and overforecasted when from the north (light winds at night).

Caveat Emptor! The high variability observed in both observed and model averages ensures frequent exceptions to these trends.

VI. DISCUSSION AND SUMMARY

A. ERROR GROWTH AND THE DIURNAL CYCLE

1. The Diurnal Cycle

Most of the mesoscale processes observed in this study were weakly forced, namely in the form of mountain-valley and thermally forced circulations between the sea and differentially heated land surfaces.

TAMS/RT captures the basic diurnal pattern, but variations between model and observed surface heat fluxes over land create and sustain errors throughout the forecast period. These errors are greatest during the warming cycle and lower during the cooling cycle and are independent of analysis error or forecast time. They are largest over inland areas. When a 12-hour forecast is used as a background field for the following analysis, these errors are carried into the next model run. A 00z 12-hour forecast consistently introduces relatively small errors into the next model run while 12z 12-hour forecasts introduce relatively large errors. Thus, the repetitive nature of error growth/decay continues in conjunction with the diurnal cycle.

Other mesoscale phenomena (mountain-valley circulation, cold air damming, etc.) also contribute to error growth, especially inland. Smoother-than-real model topography and inaccurate model elevation contributes to the wind and temperature error distribution. Model elevation that is more or less than reality creates a different diurnal temperature pattern than observed which in turn creates a different wind field.

2. Error Growth

In this study, we did not observe standard error growth with respect to time as expected from predictability theory (Anthes 1986). With relatively large initial errors, we observed no error growth over the 24-hour forecast cycle.

Anthes (1986), reports that he and other researchers have also found no error growth using limited area models.

Using time series, we observed large and small-magnitude errors. Large-magnitude error occurred three times during the study, two of which persisted throughout the forecast. In each of those cases, there was a relatively good synoptic fit between forecast and verifying analysis with no indication of high mesoscale errors. Small-magnitude error occurred day to day and is related to the diurnal cycle. Specifically, we examined 00z and 12z model run error and found there is a distinct, repetitive pattern to error growth/decay that is related to diurnal warming and cooling over land. Also related to the diurnal cycle is the pattern of model and observed variability.

Data assimilation can reduce or increase error depending on the quality of the data, time of day, and region within the domain. Data assimilation can introduce large-magnitude errors into the analysis disrupting any mesoscale definition contained in the background field. In one such case, we observed a reduction in forecast error at one location while at another, error increased for one variable and decreased for another. This example highlights some of the complexities involved in using mesoscale models and how forecasters and researchers need to re-characterize the meaning of an "improved" forecast to mirror the high-variability on the mesoscale and to assess dynamically important errors.

A poorly defined background field can also introduce large-magnitude errors into the analysis following a cold start. Sometimes TAMS/RT uses a 12-hour NOGAPS forecast, other times it uses a 24-hour COAMPS forecast. On one hand, in a synoptically forced situation, a NOGAPS forecast probably has a better depiction of large-scale features (fronts, etc.). On the other hand, a 24-hour COAMPS forecast will contain more mesoscale detail than NOGAPS with about the same magnitude of error as a previous COAMPS 12-hour forecast would have had. In a weakly forced scenario and in the absence of a previous

12-hour forecast, a 24-hour COAMPS forecast with its highly developed mesoscale structure, should be the background field of choice.

Warner (1992) and Sashegyi and Madala (1992) feel that local forcing can reduce error if the surface parameters are accurately specified and could increase the error if poorly specified. Anthes (1986) felt that mesoscale simulations are insensitive to random fluctuations in the initial wind, temperature, and moisture fields. Instead, he believes they are more sensitive to errors in the large-scale flow and to model physics. The large-magnitude errors we observed were associated with system crashes, data assimilation, and poor background fields. The small-magnitude errors may have been related to model parameterizations (surface heat fluxes) and model elevation differences. Since we did not observe error growth and we believe that small errors do indeed grow, we assume that the limitations of present day numerical mesoscale models and data assimilation techniques inhibit observation of random day to day wind and temperature fluctuations within a highly variable, weakly forced environment. In other words, using these tools in this environment, we have no mesoscale analysis skill.

3. Error Pattern and the Diurnal Cycle: The Link

TAMS/RT error growth and decay are closely linked to the diurnal cycle. Model inconsistencies that follow, but inaccurately capture the diurnal cycle, ensure that small-magnitude errors are sustained through the forecast. When used as a background field for a warm start, those errors are carried into the following model run. The diurnal cycle and repetitive nature of the error pattern ensures that large-magnitude errors, regardless of model run, eventually return to the norm. Poor data assimilation and/or background field can delay that return.

Figure 7 shows that when compared to observed mean values, wind errors account for a large contribution to the observed mean wind. Temperature errors meanwhile, account for a smaller error contribution. The synoptic scale

west/east geostrophic pressure gradient explains why mean observed and error values for east/west wind (u) are higher than north/south (v). Also, it may explain why errors are higher during the warming cycle (daytime) when higher inland temperatures drive strong onshore westerly winds that interact with coastal topography and generate a complex inland wind flow with high variability and thus, high error. At night, inland areas cool and a stable boundary layer forms. Wind flow is light and less variable (i.e., interacts less with topography) and results in lower errors. Any variations between model and actual topography accentuate the error.

B. THE FORECASTING CHALLENGE

How does a forecaster adjust a mesoscale forecast using an analysis embedded with relatively large errors? Does the traditional comparison of analysis with satellite, previous model run, other models, or even observations really help?

There are some clues. An analysis that is smoother than the previous 12-hour forecast probably has large-scale errors. Nonetheless, even a well-defined mesoscale analysis will have errors and in a weakly forced mesoscale environment and those small-magnitude errors (especially wind) are relatively large compared to observed mean values.

The challenge lies in understanding error and its relationship to:

- Cold versus warm starts. Both can introduce large-magnitude errors depending on quality of background fields and data assimilation. A cold start may be better in a strongly forced synoptic situation while a warm start may be preferable in a weakly forced one. Ideally, the forecaster should be able to decide which initialization scheme to use depending on the current synoptic trends, i.e., wintertime with frequent frontal passages, or summertime with light forcing and mesoscale influence.

- Background fields. As noted above, in a weakly forced environment, a 24-hour mesoscale forecast with high-resolution mesoscale structure may be preferable to a smoother 12-hour global scale forecast.

- Data assimilation. The true nature of the data assimilated into a particular model run is unknown to the forecaster. Depending on quality of data, it can greatly influence the magnitude of the analysis and forecast errors within all or part of the domain, sometimes or all the time.

- Model physics and parameterization inaccuracies. Elevation differences between model and reality can account for diurnal inaccuracies in model temperature and wind fields. In a certain season, a simple temperature correction may actually degrade the forecast.

C. AREAS FOR FURTHER STUDY AND RECOMMENDATIONS

Based on our findings, we believe the following areas warrant further consideration.

1. Continue to Collect Fall and Winter Error Statistics for NMPOC San Diego.

Error may increase or decrease under strong synoptic forcing. Regardless, will the diurnal error pattern still be evident?

2. Evaluate the Average Trends We Observed at Other Locations.

Different locations may have similar tendencies. We recommend collecting statistics for those locations and assessing average trends. In this manner, a large database can be constructed that highlights model tendencies in certain areas during certain conditions and times. For example, errors due to model inconsistencies in following the diurnal cycle may be quite similar in areas around the Mediterranean and Persian Gulf. This could lead to a similar error

pattern at inland areas during the height of daytime or seasonal heating than we observed.

3. Reevaluate Data Assimilation Schemes.

Data assimilation with NMPOC's TAMS/RT varies daily and its forecast impact is difficult to assess. Better documentation of the data that is assimilated along with the influence of different types of data and their impact on analysis and forecast error is needed.

For example, under the present scheme does initializing a model run with few or even several local surface observations make a difference? Approximately 800 to 1500 NOGAPS pseudo-raob data points are assimilated into each run. This may be introducing NOGAPS bias into the mesoscale forecast. Hovermale (1986) feels that any smoother, larger scale circulation analyzed aloft will quickly destroy or rearrange any fine detail introduced into the initial conditions at the surface alone.

4. Evaluate the Effects of Lateral Boundary Conditions.

The influence of lateral boundary conditions (LBC) on the inner nest is unclear. A better understanding of LBC error contribution, if any, is needed.

NOGAPS lateral boundary conditions update TAMS/RT every 12 hours (tau 12). We report one case (April) where the forecast changes notably in six hours even though only very limited data assimilation (pseudo-raobs only) took place. This change could have been due to model physics or the pseudo-raobs, but it also may be possible that insufficient spacing from the mother grid allowed lateral boundary conditions to influence the inner nest.

5. Account for Large Analysis Error.

We have showed that the analysis contains relatively large errors when compared to mean observed values. These large errors can degrade the TAMS/RT NOWCAST analysis, which is a mesoscale analysis with the best estimate of current environmental conditions within the domain (NRL TAMS/RT webpage 1999). It is designed to assist the tactical forecaster with critical

forecasts. For example, in a light wind scenario, if 33 knots of relative wind are required to recover aircraft and the ship can only maintain 30 knots of speed. A 1-2 m/s (2-4 knots) error from an unexpected direction can be detrimental. During the day, we've shown analysis error values up to 1 m/s (2 knots) that comprise 26 to 36% of the mean observed values. At night those values change to 0.5 m/s (1 knot) or 147 to 300% of the mean observed value!

In view of large-scale data assimilation that might be occurring, updating TAMS/RT with local observations may have little affect.

6. Establish a TAMS/RT Working Group at NPS and NRL

Installation of TAMS/RT at various sites is well underway. We recommend statistical analysis of areas of forecasting interest in order to determine and quantify average trends. Manpower and technical ability limits this type of analysis at Naval METOC Centers. We have shown that there is much to learn about mesoscale model forecasting and data assimilation that needs to be done in a research environment rather than in the field.

NPS and NRL can work in concert to collect, analyze, test, recommend and implement changes that will improve our ability to serve the fleet.

THIS PAGE INTENTIONALLY LEFT BLANK

APPENDIX A. TABLES

The following pages of tables are grouped together in this appendix to help make reading them easier.

Table I: COAMPS General characteristics and specific configuration for NPMOC San Diego's TAMS-RT. From ref. [Reiss 1999].

QUALITY CONTROL	
Observations	Algorithms for atmospheric observational data (Baker 1992).
ANALYSIS	
Levels	Analysis on 16 standard pressure levels (1000 MB to 10 MB).
Synthetic observations	Synthetic observations from NOGAPS in data sparse regions.
First-guess fields	• NOGAPS for cold starts, • COAMPS for warm starts (data assimilation)
MVOI of winds and heights	Lorenc technique (1986) for mapping obs to the model grid(s).
Volume method	Adjustable volume size for a separate analyses on each nested grid
Input	Synoptic, ship, bathymetric, ice, radiosondes, pibals, AIREPS, ACARS, SSMI, surface and cloud track winds, and synthetic observations.
D-values/Thickness	Radiosondes, DMSP, NOAA satellite.
Superobs	Aircraft and SSMI.
Univariate Analysis of Temperature and Dew-point depression	Cressman (1959). Radiosonde and synthetic observations only with gross-error checking.
ATMOSPHERIC MODEL	
Dynamics, Numerics:	
Equations	• Non-hydrostatic compressible equations (Klemp and Wilhelmson 1978). • Equations also include map factors, terrain, lateral, lower, and upper boundary conditions and are solved using a combination of finite differencing, finite elements, and spectral methods. • Time-splitting method in horizontal allows large time steps for slow modes and small time steps for fast modes. Semi-implicit method in vertical.
Diffusion	Horizontal diffusion (4^{th} order difference method) is used to control spurious, high frequency waves that are not important for the final solution.
Grid configuration	• Staggered C grid (Arakawa and Lamb (1977)) • Multiple nested grid options.
Vertical coordinates	Terrain following coordinate (sigma z; Gal-Chen and Somerville 1975) allows flow over an irregular surface.
Vertical levels	• 30 sigma levels (m) with higher density in lower troposphere • Levels at (m): 10, 30, 55, 90, 140, 215, 330, 500, 750, 1100, 1600, 2300, 3100, 3900, 4800, 5800, 6800, 7800, 8675, 9425, 10175, 10925, 11675, 12425, 13300, 14300, 16050, 19400, 24400, 31050. • Note: TAMS-RT allows the user to change the vertical coordinate system from these default values.
Grid projection	Lambert conformal, mercator, or spherical.
Mesh ratio	3:1
Grid spacing	• Synoptic to LES. • Note: NPMOC San Diego's TAMS-RT settings for thesis case studies were 45, 15, and 5 km's (coarse/medium/fine).

Precipitation Physics	
Grid spacing ≥ 10km	• Stratiform: Explicit moist physics (Rutledge and Hobbs 1983). • Convective: Kain and Fritsch (1993) cumulus parameterization.
Grid spacing < 10km	• Rutledge and Hobbs (1983) explicit moist physics for both stratiform and convective clouds and precipitation . • For grid resolutions < 10km, COAMPS is effectively acting as a cloud model.
Options for COAMPS SP (simplified physics)	• Stratiform: Instantaneous condensation/fallout. • Convective: Kuo (1974) cumulus parameterization. • Note: NPMOC San Diego's TAMS-RT did not employ SP.
Known characteristics	• Kain and Fritsch: under-predicts and noisy over ocean • Kuo: over-predicts, dependent upon grid resolution, and 3-5 times faster than KF.
Radiation	Radiative transfer parameterization (Harshvardan et al. 1987)
Boundary layer and surface parameterizations	
Land-use Surface albedo Surface roughness Ground wetness Ground temperature SST	• Initially taken from a global monthly climatology database (resolution ~ 1° lat) and thereafter from the previous forecast. • In certain regions, USGS 1-km global land-use database remapped to 0.01° resolution replaces climatology fields. • Look up table assigns each land-use type (1-94) a value of ground wetness, albedo (open sea = 0.09; ice = 0.6), and surface roughness based primarily on Henderson-Sellers and Wilson (1986). Values are averaged at 0.01° resolution over each of the COAMPS domains to determine one value of each for every COAMPS grid point. • Note: NPMOC San Diego's TAMS-RT now uses a 1-km global land-use database and a CODA SST and ice analysis updated twice daily. This value is held constant throughout each forecast cycle.
Turbulence	1.5 order, level 2.5 TKE Closure (Mellor and Yamada 1982)
Surface Layer	Louis scheme (1979).
Terrain and coastal source and resolution	• Grid spacing ≥ 20km: Uses 20-km terrain database bilinearly interpolated to the grid resolution. • Grid spacing < 20km: Uses 1-km terrain database (NIMA level 1) bilinearly interpolated to the grid resolution. • Terrain matching employed across mesh boundaries. • Note: NPMOC San Diego's TAMS-RT uses 1-km global terrain and 400-m coastal databases.
Lateral Boundary Conditions	
Time dependent boundary conditions	Davies (1976) or optionally Perkey-Kreitzberg (1976) interpolated from NOGAPS (16 or 21 levels) available in temporal resolutions of hourly or in multiples thereof. Options for periodic, radiation, or fixed in idealized simulations. Option for sub-nesting local COAMPS domains within coarser regional domains. Note: NPMOC San Diego uses Davies method, 16-level, 12-hour temporal resolution lateral boundary conditions (LBCs) from NOGAPS. COAMPS is typically triply nested and the LBCs of the inner meshes are updated at the model time step. Only the outer coarse mesh "sees" the NOGAPS LBCs.

Table II. Outer nest (45 or 54 km) surface pressure comparison between verifying analysis and 00z and 12z model run forecasts (f12 and f24) for best fit over SOCAL area.

00Z model run	*#of times f12 has lower pressure, VT: 12z*	*No. cases*	*#of times f24 has lower pressure, VT: 00z*	*No. cases*	*f24 better fit than f12*	*No. cases*
MAY	100.00%	9	66.00%	9	55.00%	9
JUN	100.00%	8	88.00%	8	66.00%	9
JUL	100.00%	18	74.00%	19	77.00%	17
AUG	92.00%	13	62.00%	13	73.00%	11
SEP	87.00%	15	23.00%	13	54.00%	13
Ave	**95.80%**	63	**62.60%**	62	**65.00%**	59
Stdev	6.02%		21.70%		10.37%	

12Z model run	*#of times f12 has lower pressure, VT: 00z*	*No. cases*	*#of times f24 has lower pressure, VT: 12z*	*No. cases*	*f12 better fit than f24*	*No. cases*
MAY	25.00%	8	100.00%	7	100.00%	7
JUN	78.00%	9	100.00%	8	100.00%	7
JUL	35.00%	17	100.00%	13	94.00%	17
AUG	25.00%	12	89.00%	9	90.00%	10
SEP	25.00%	8	86.00%	7	87.00%	8
Ave	**37.60%**	54	**95.00%**	44	**94.00%**	49
Stdev	23.00%		6.93%		5.61%	

Table III. Inner nest relative error (bias) contribution to mean observed values of u, v, and T for analysis (f00) of each model run.

Variable per model run	*Average observed*	*Average Error (bias)*	*Average RMS Error*	*% Contribution*
U_00z	3.68 m/s	0.97 m/s	2.71 m/s	26%
U_12z	0.40 m/s	0.59 m/s	2.48 m/s	147%
V_00z	0.81 m/s	0.29 m/s	2.44 m/s	36%
V_12z	-0.19 m/s	0.56 m/s	2.48 m/s	-294%
T_00z	21.68 °C	2.72 ° C	4.53°C	13%
T_12z	15.18 °C	0.58 °C	3.57°C	4%

Table IV. Average observed and model east/west (u) and north/south (v) wind vector direction and corresponding average wind direction and speed for the inner nest. Double arrows indicate greater value in order to assess if model is over or underforecasting winds.

Forecast by Model Run	*Observed vector direction u, v*	*Model vector direction u, v*	*Observed direction (°True) speed (m/s)*	*Model direction (°True) speed (m/s)*
00z Model				
U_f00	→→	→	258	259
V_f00	↑↑	↑	3.77	2.77
U_f06	→→	→	278	291
V_f06	↓	↓↓	1.25	1.05
U_f12	→→	←	295	193
V_f12	↓	↓↓	0.44	0.68
U_f18	→→	→	244	256
V_f18	↑↑	↑	2.04	0.90
U_f24	→→	→	258	258
V_f24	↑↑	↑	3.77	3.01
12z Model				
U_f00	→→	←	295	194
V_f00	↓	↓↓	0.44	0.77
U_f06	→→	→	244	255
V_f06	↑↑	↑	2.04	1.03
U_f12	→→	→	258	259
V_f12	↑↑	↑	3.77	2.97
U_f18	→→	→	278	298
V_f18	↓	↓↓	1.25	1.18
U_f24	→→	←	295	183
V_f24	↓	↓↓	0.44	0.75

Station	*Model Elevation (m)*	*Actual Elevation (m)*	*Difference*
Palm Springs (PSP)	814	141	673
Riverside (RIV)	1092	469	623
Riverside Municipal (RAL)	844	249	595
Chino (CNO)	972	188	784
Ontario (ONT)	1129	287	842
Burbank (BUR)	1057	236	821
Beaumont (BUO)	1519	692	827
Thermal Airport (TRM)	769	-36	805

Table V. Differences between model and real elevation at selected inland stations within the inner nest.

THIS PAGE INTENTIONALLY LEFT BLANK

APPENDIX B. FIGURES

The following pages of figures are grouped together in this appendix to help make reading them easier.

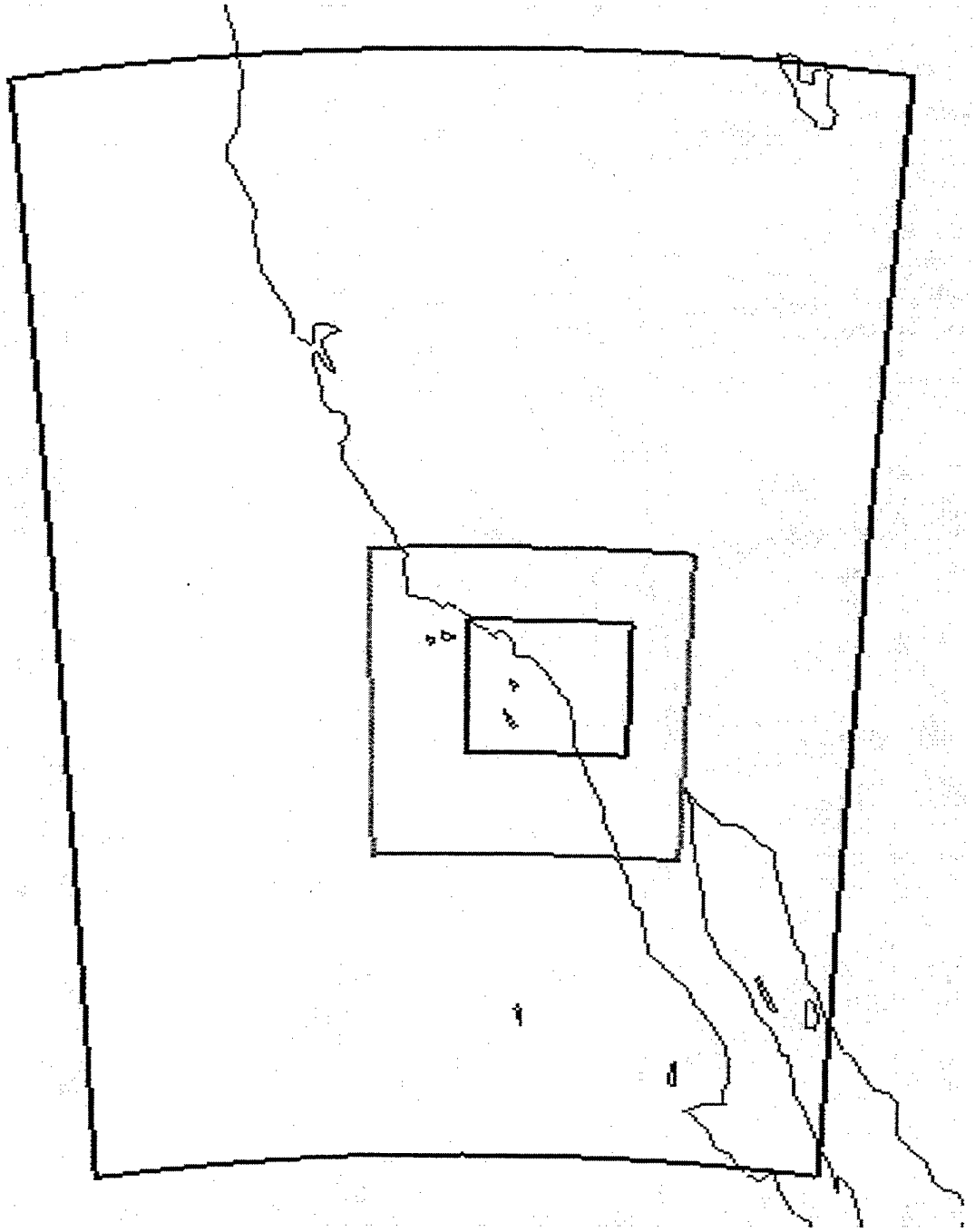

Figure 1. NPMOC TAMS/RT horizontal grid domain, 45/15/5 km. Domain sizes were changed to 54/18/6 km on 18 June 1999. From ref. [Reiss 1999].

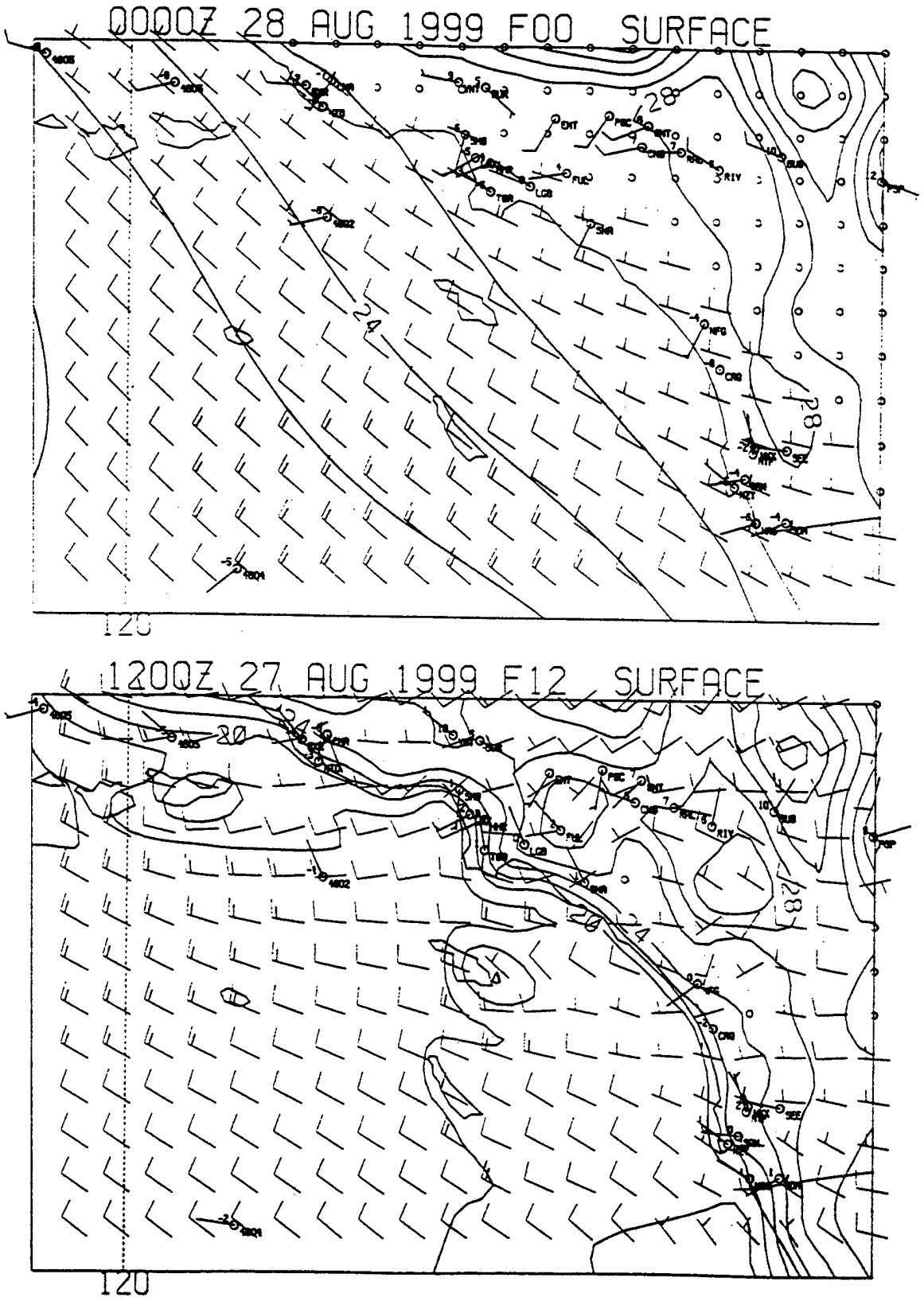

Figure 2. VISUAL plot for 27 August 12z model run, 12-hour (f12) forecast and 28 August analysis (f00). Wind in knots, temperature at 2 °C isotherms.

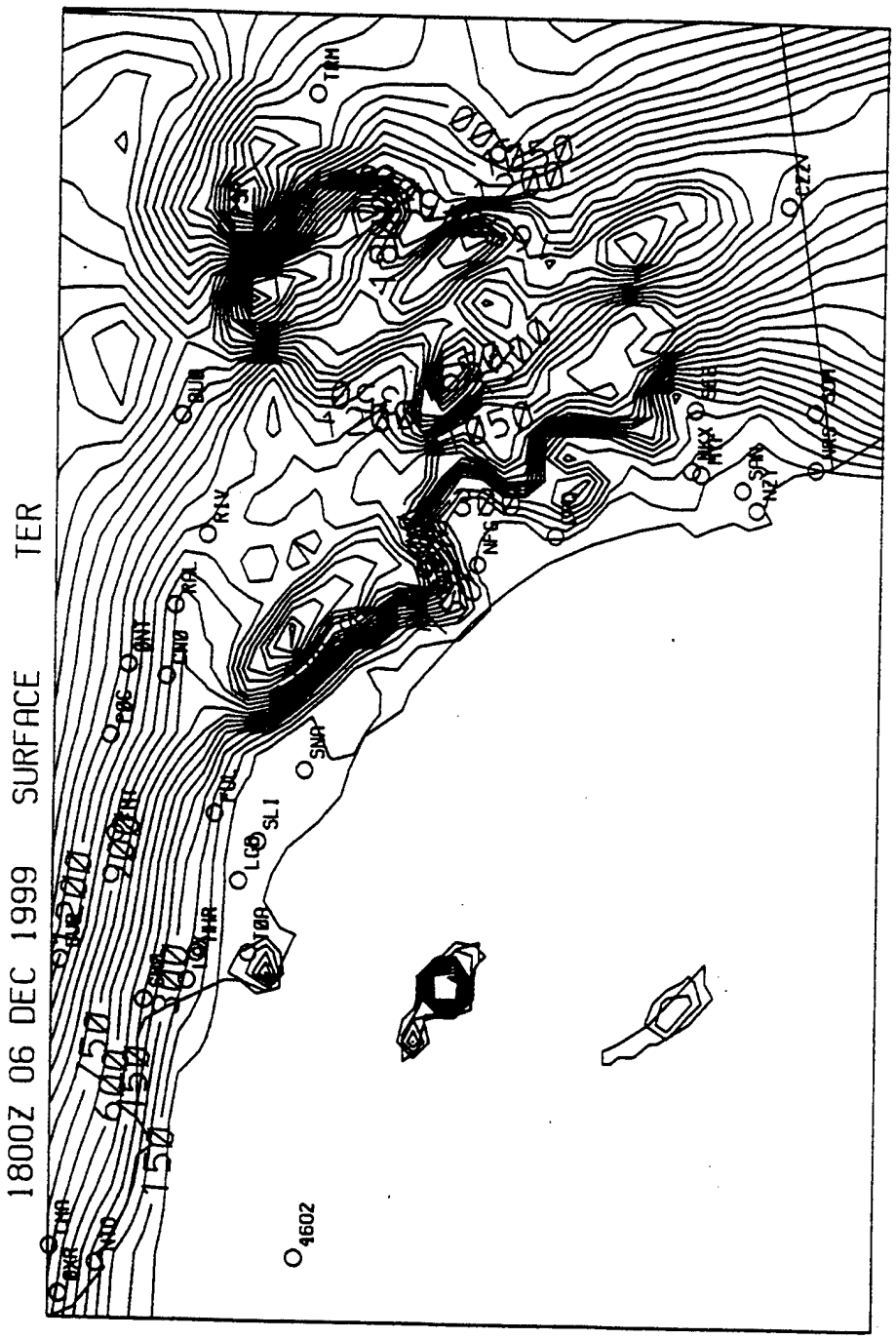

Figure 3. VISUAL plot for inner nest (5 km) depicting model topography and various reporting stations. Contour interval of 75 meters.

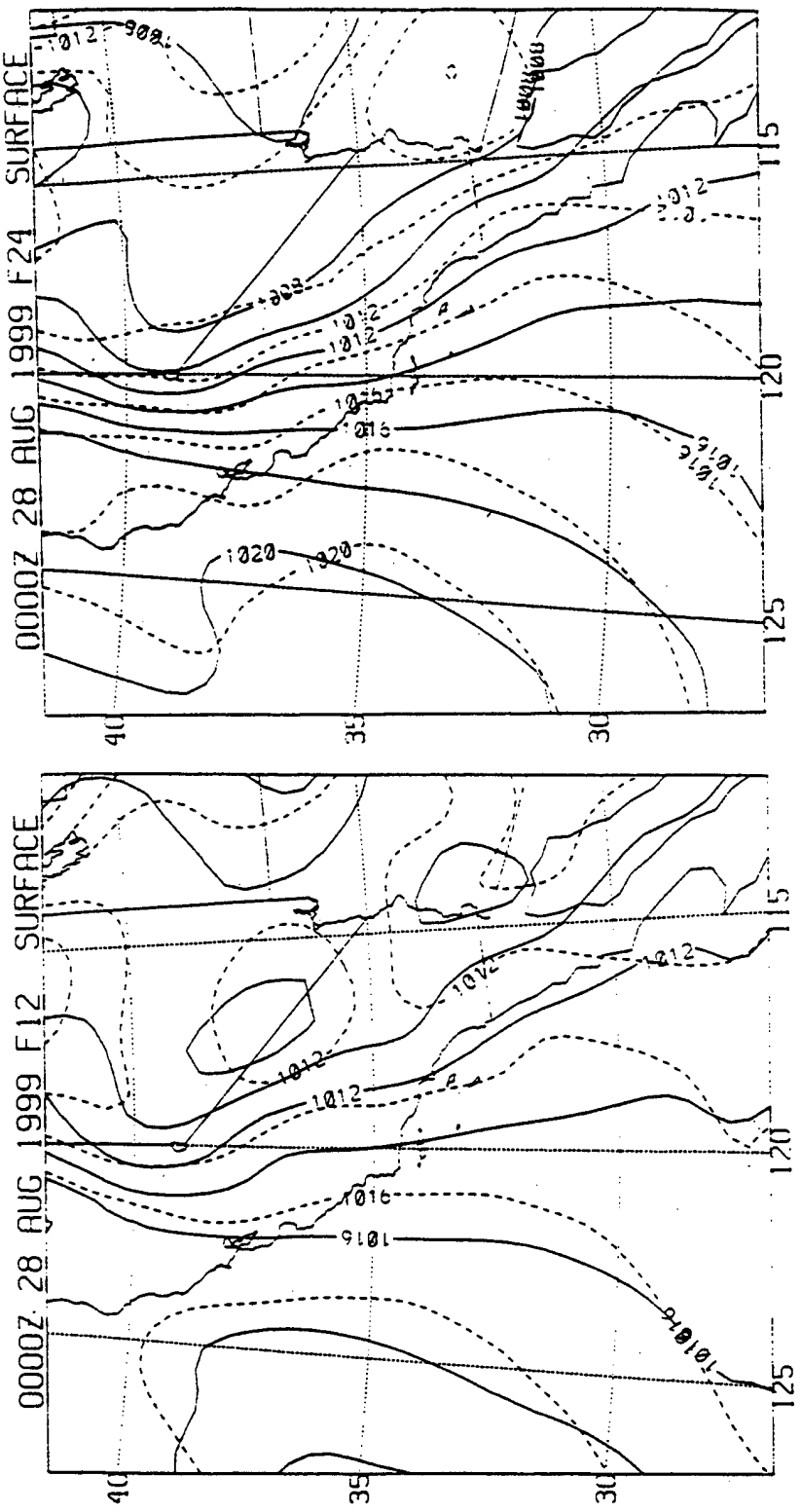

Figure 4. Outer nest (54 km) sea level pressure forecast for 28 August 00z model run, 12 and 24-hour (f12, f24). Forecast = solid, analysis = dashed line.

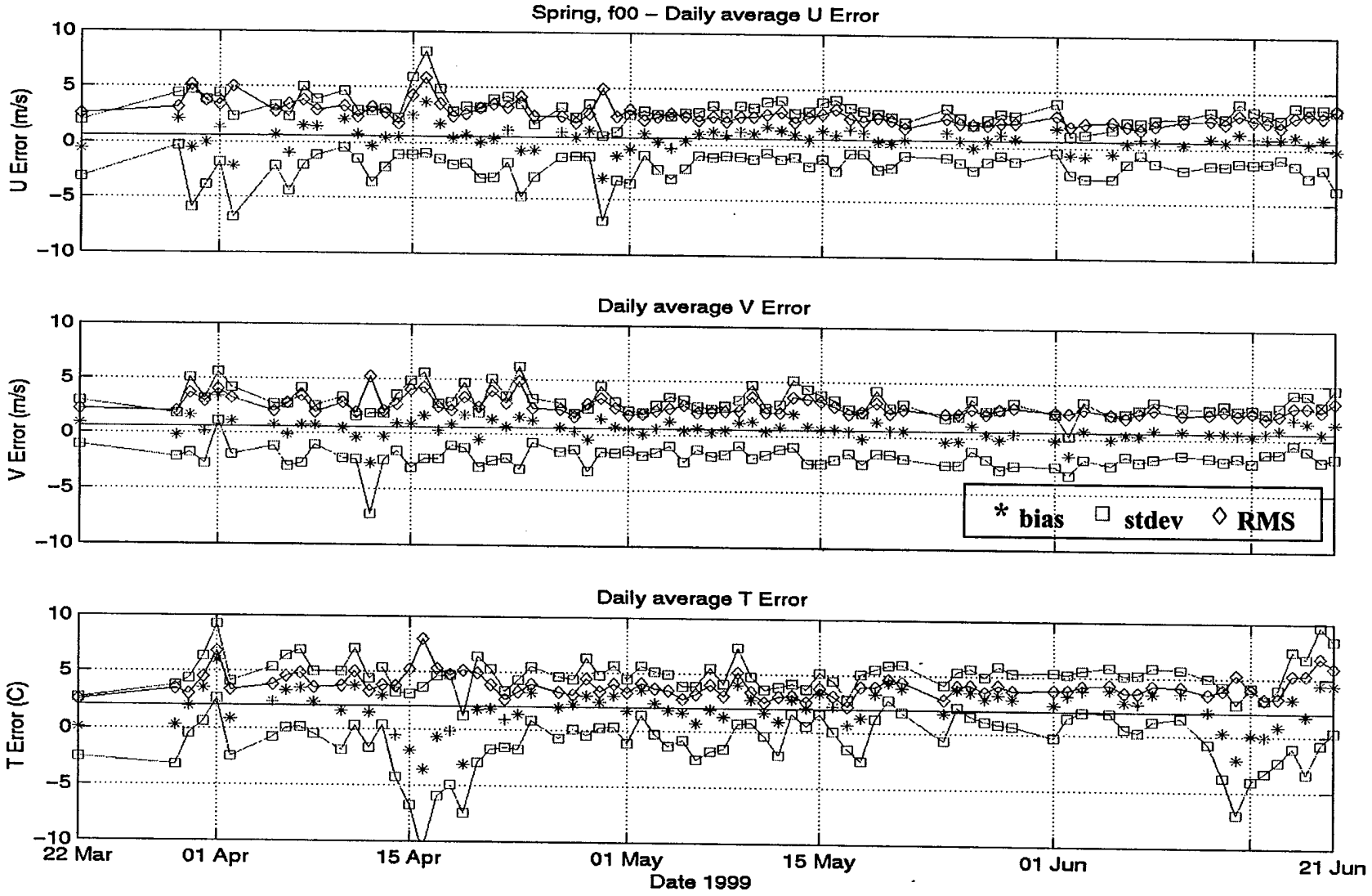

Figure 5a. Spring time series: analysis (f00).

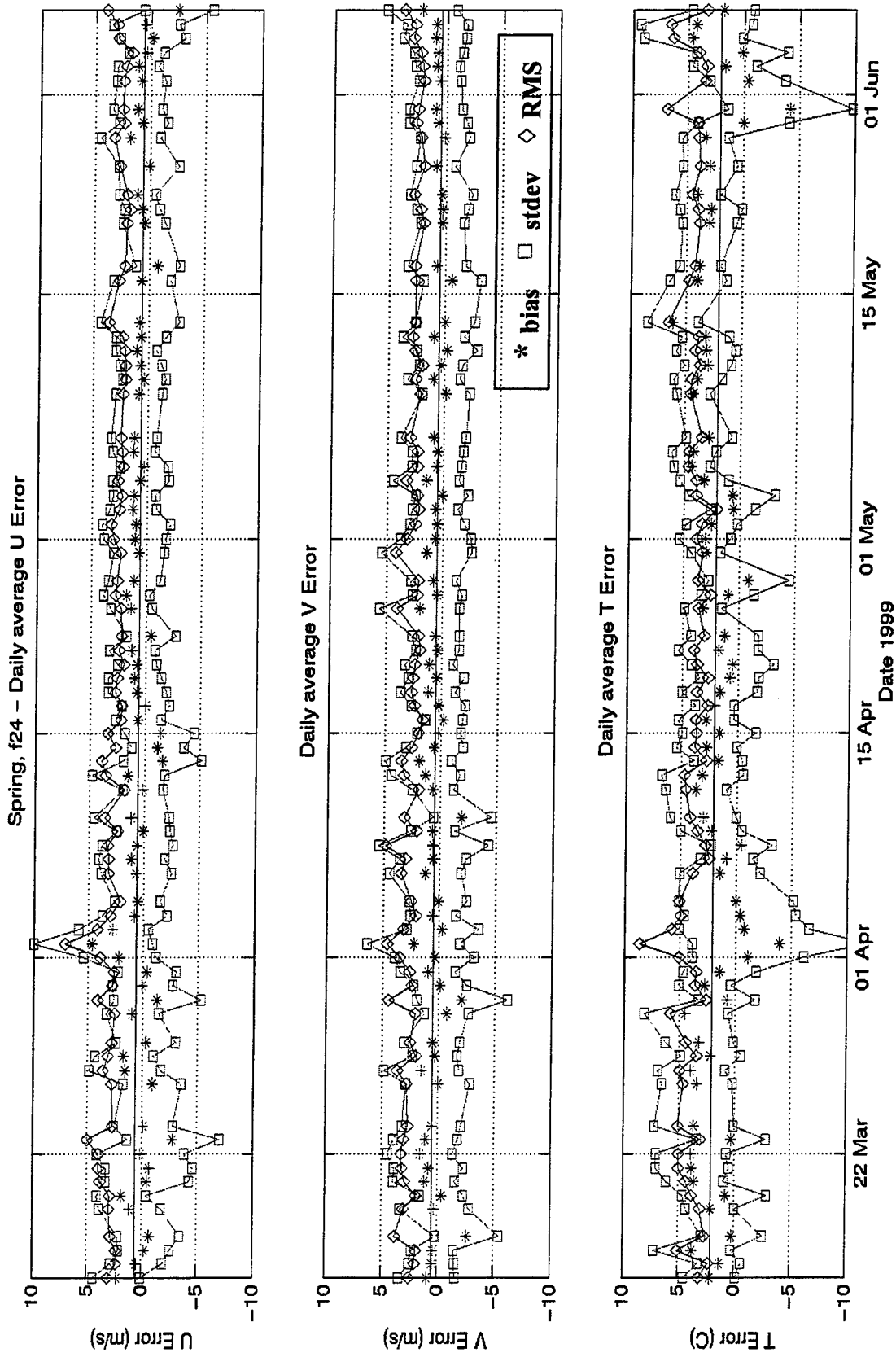

Figure 5b. Spring time series: 24-hour forecast (f24).

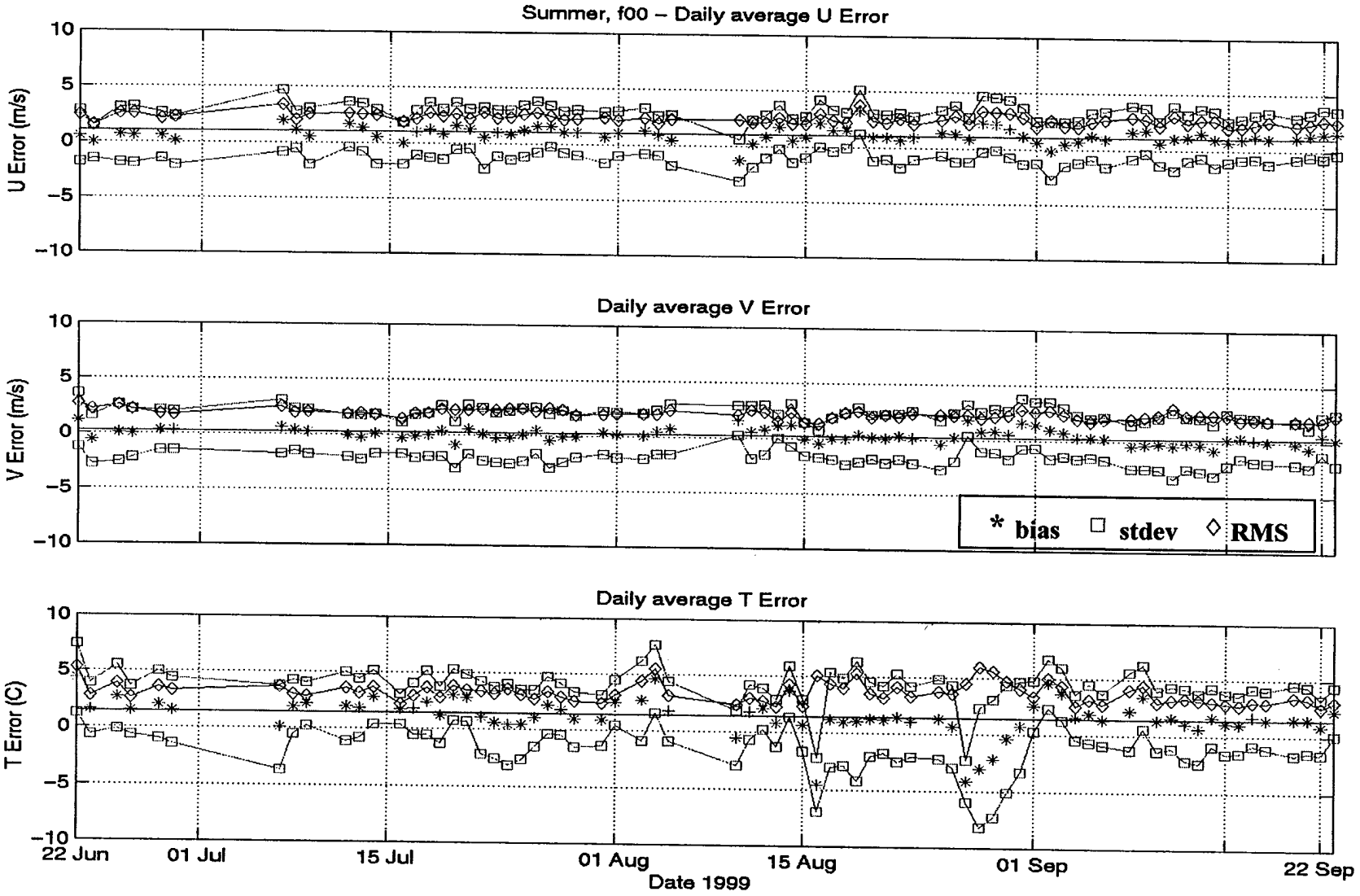

Figure 5c. Summer time series: analysis (f00).

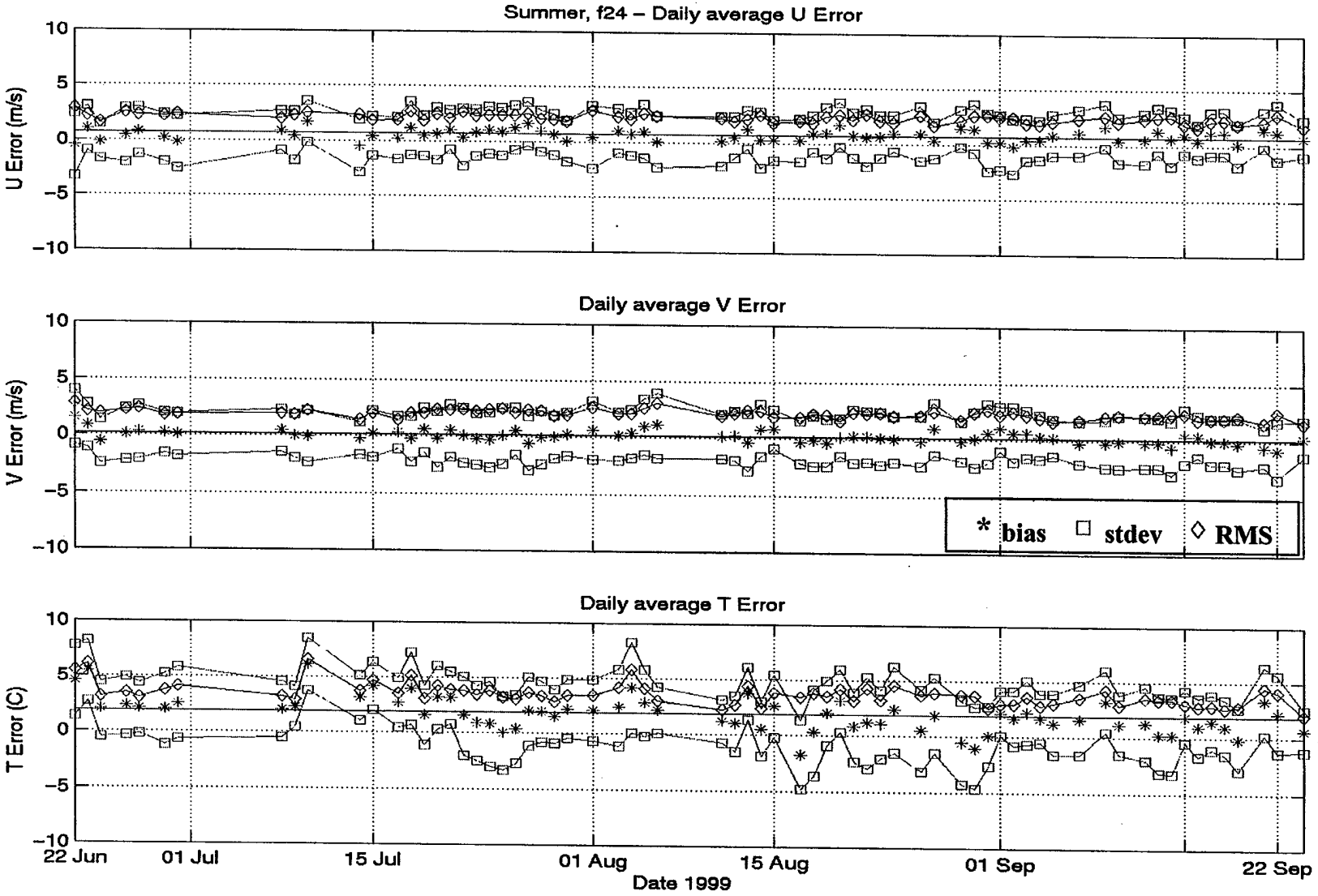

Figure 5d. Summer time series: 24-hour forecast (f24).

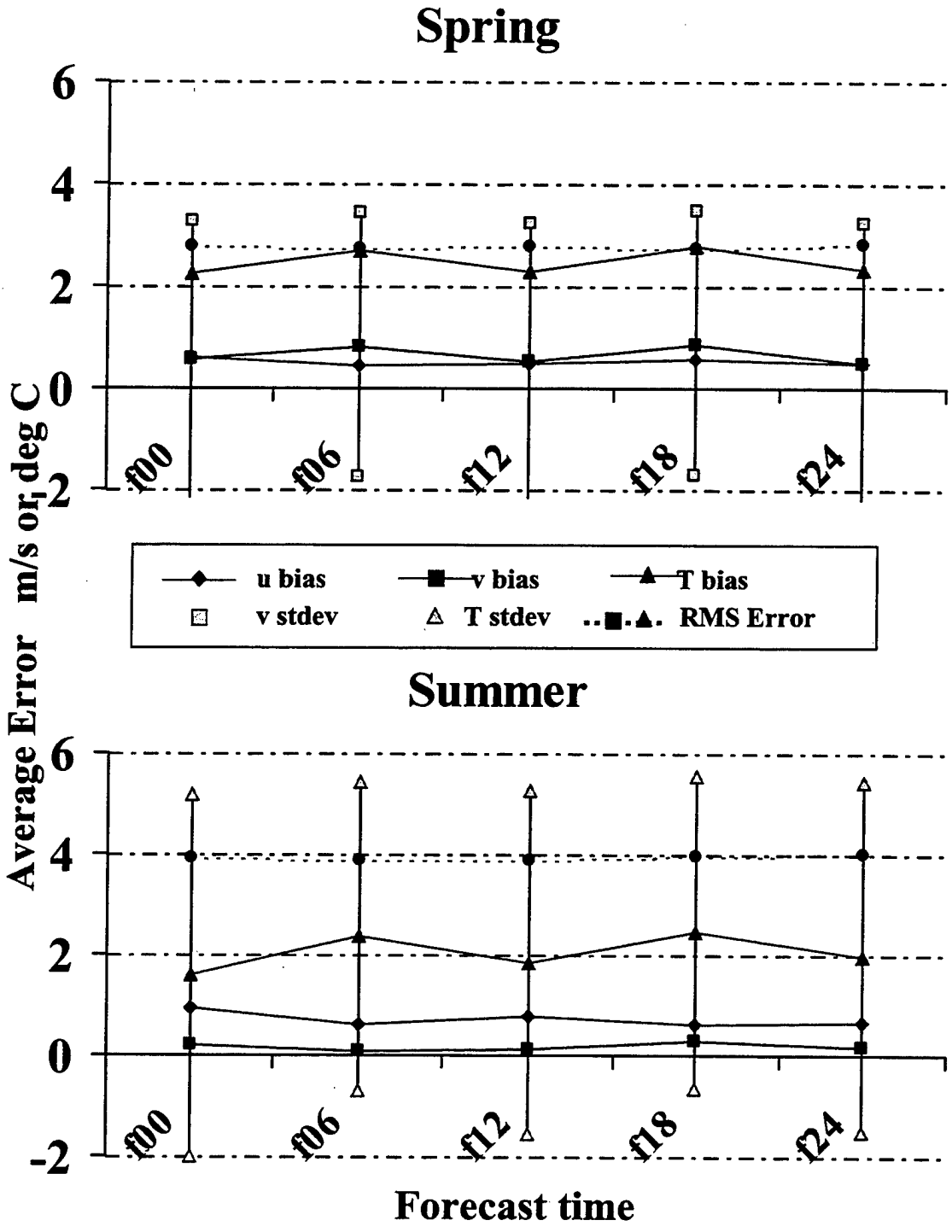

Figure 6. Inner nest forecast cycle error growth for spring and summer. Error bars are shown for spring v vector, and summer temperature only (other variables have similar magnitudes)

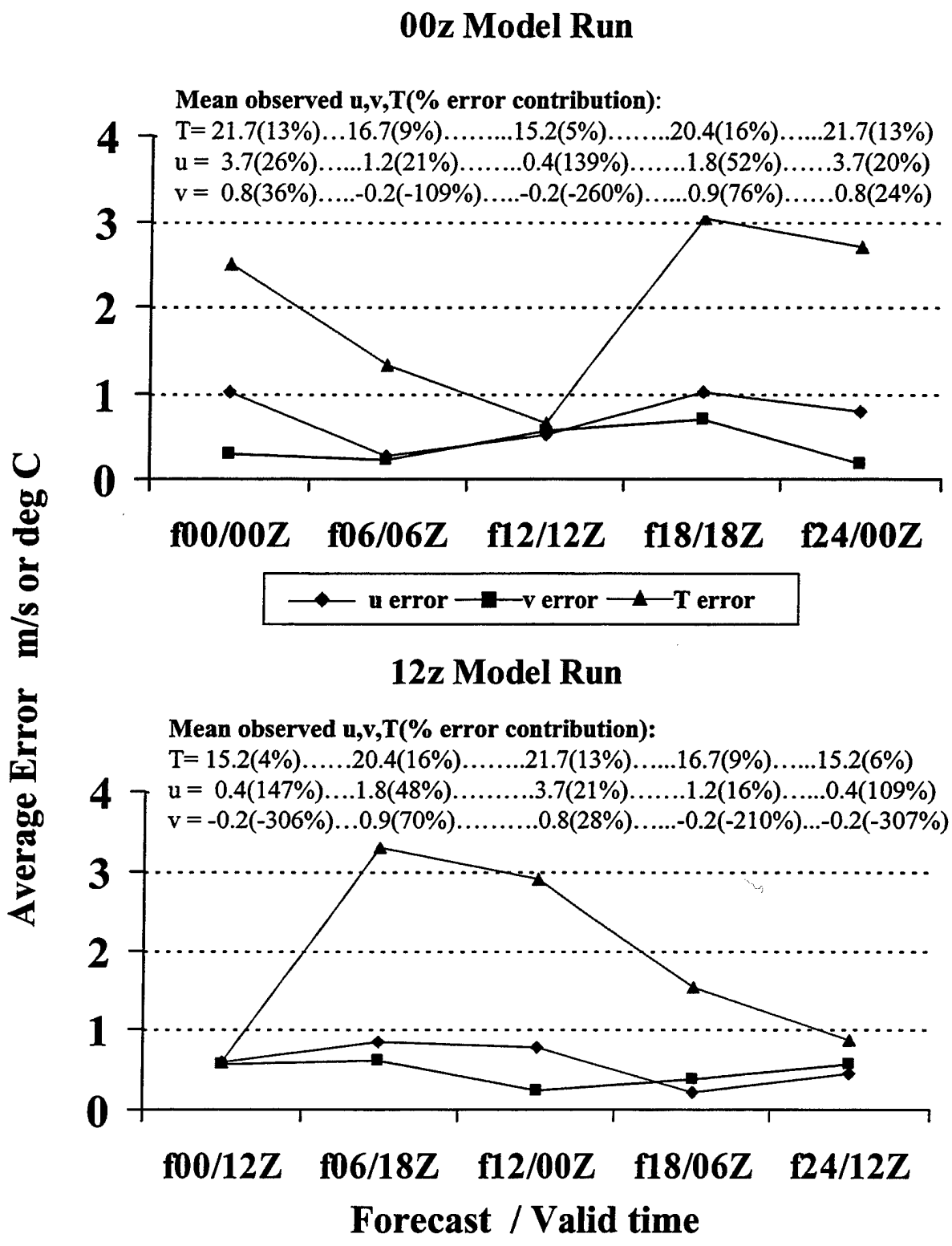

Figure 7. Error growth by model run for inner nest. Mean observed values of u, v, and T are given to show relative contribution of error.

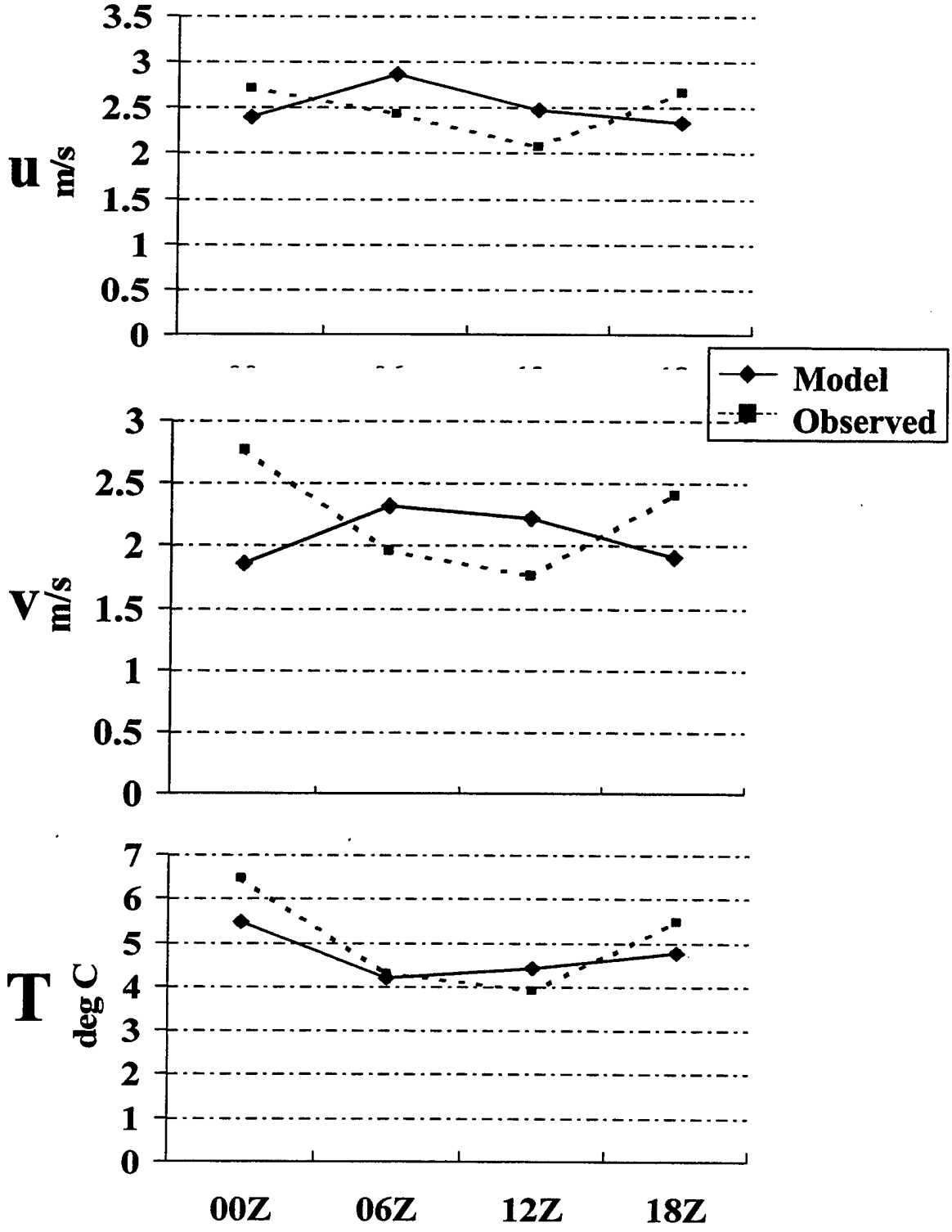

Figure 8. Model versus observed average variability for the inner nest.

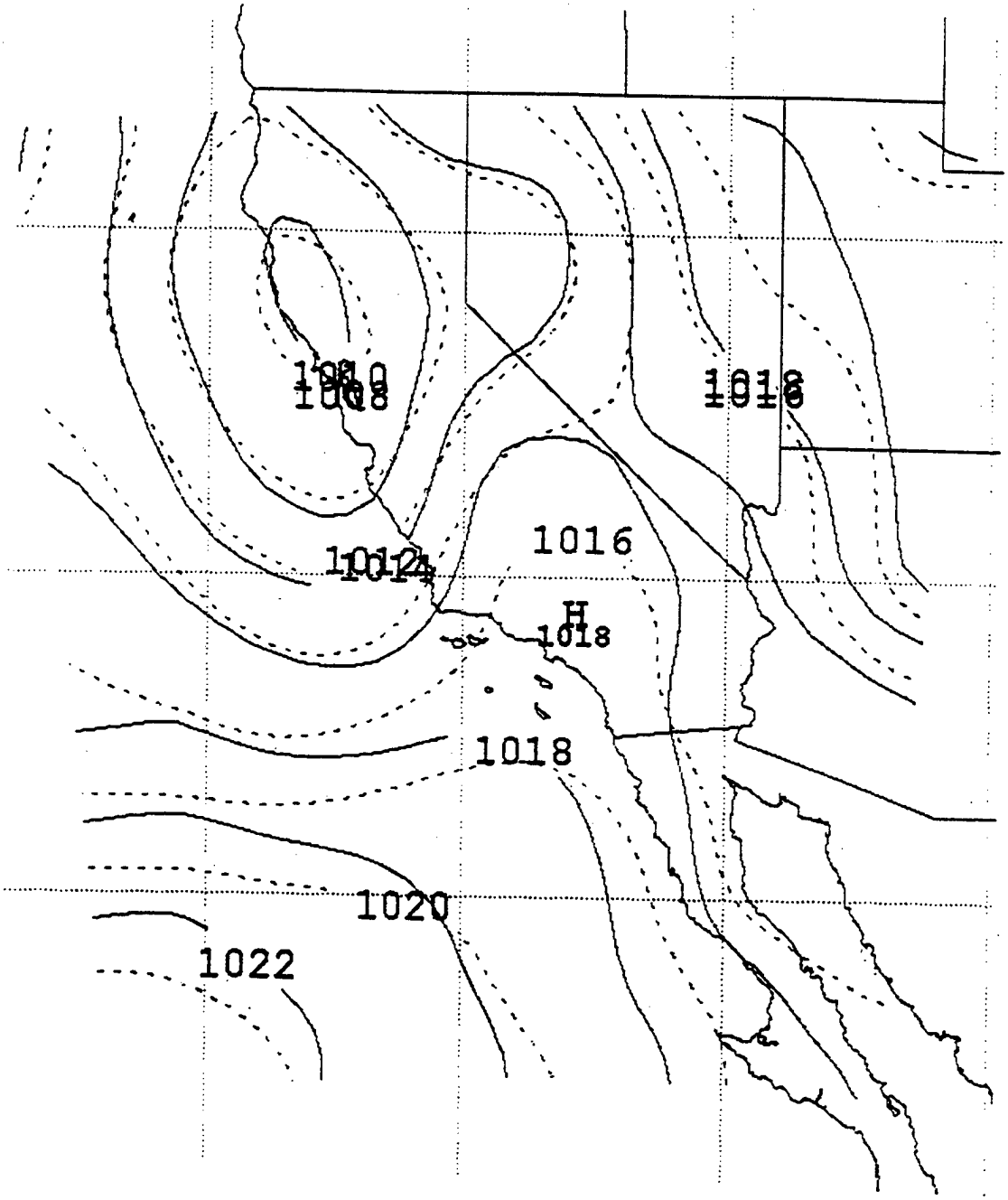

Figure 9. Outer nest (45 km) sea level pressure forecast for 11 April 00z f12 (12-hour forecast = solid line), and model analysis for 11 April 12z f00 (dashed line). Contour interval = 2 mb.

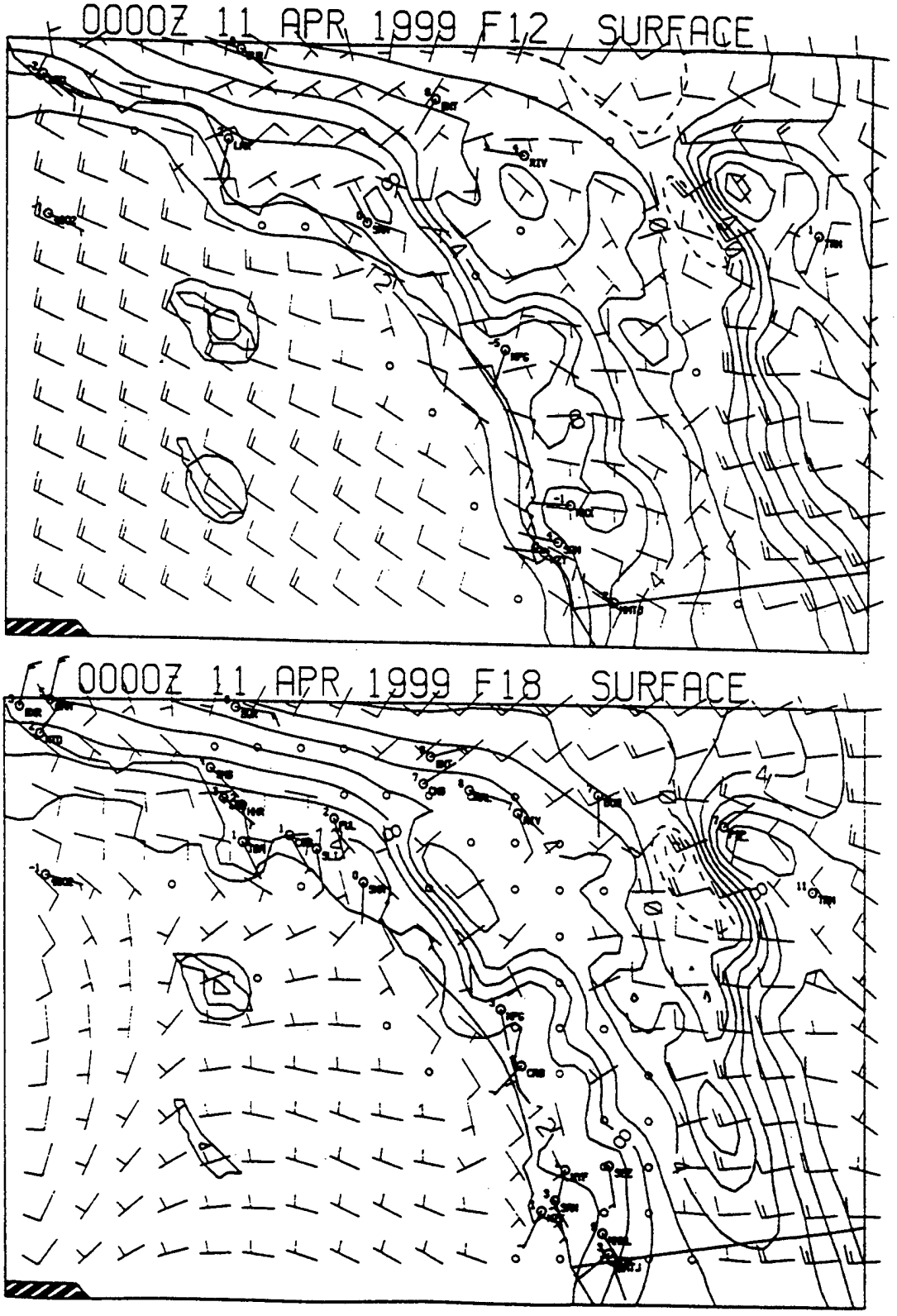

Figure 10. VISUAL plot for inner nest, 11 April 00z model run, 12 and 18-hour forecast (f12 and f18). Contour interval of 2 °C.

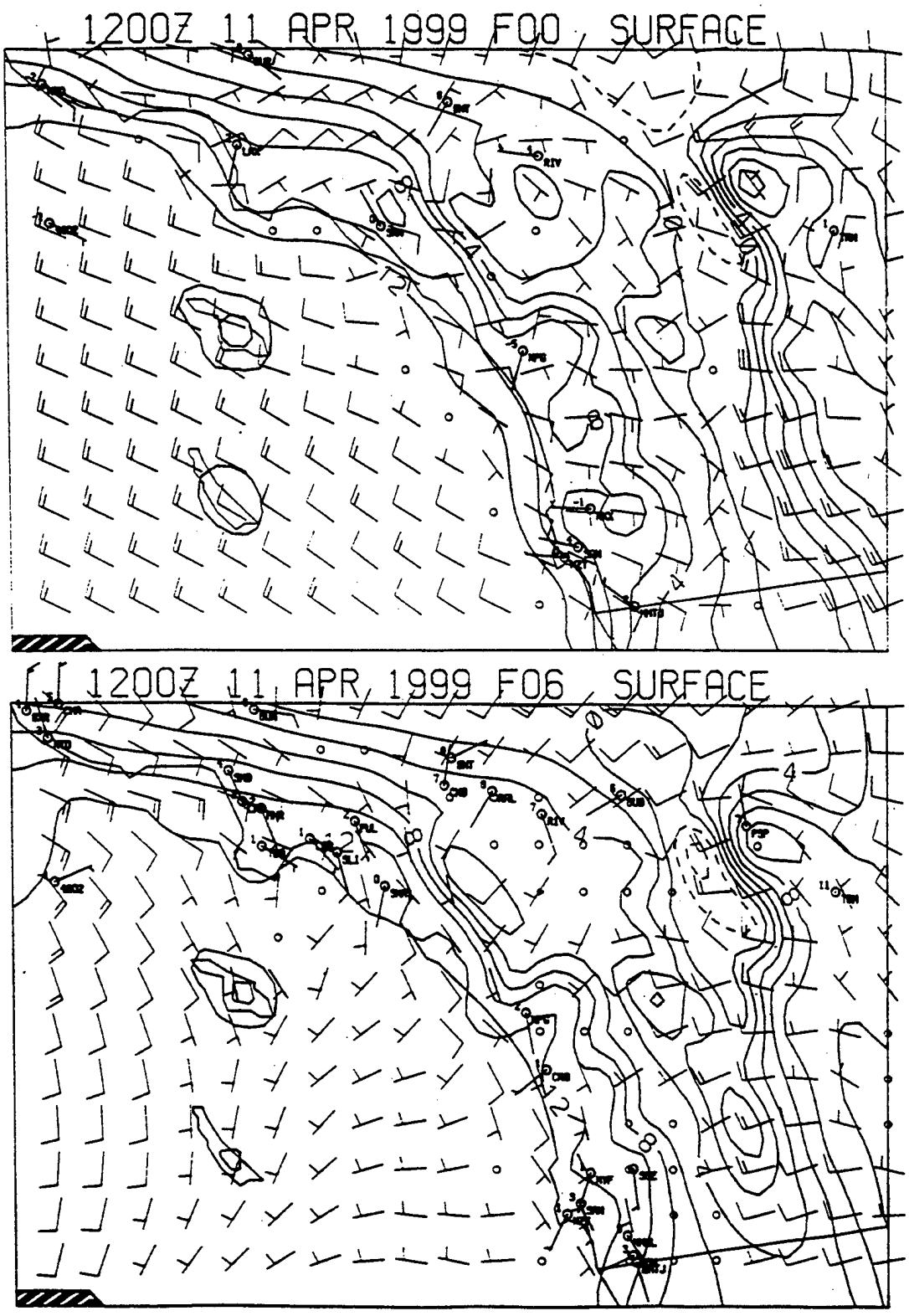

Figure 11. VISUAL plot for inner nest, 11 April 12z model run, analysis and 6-hour forecast (f00 and f06). Contour interval of 2 °C.

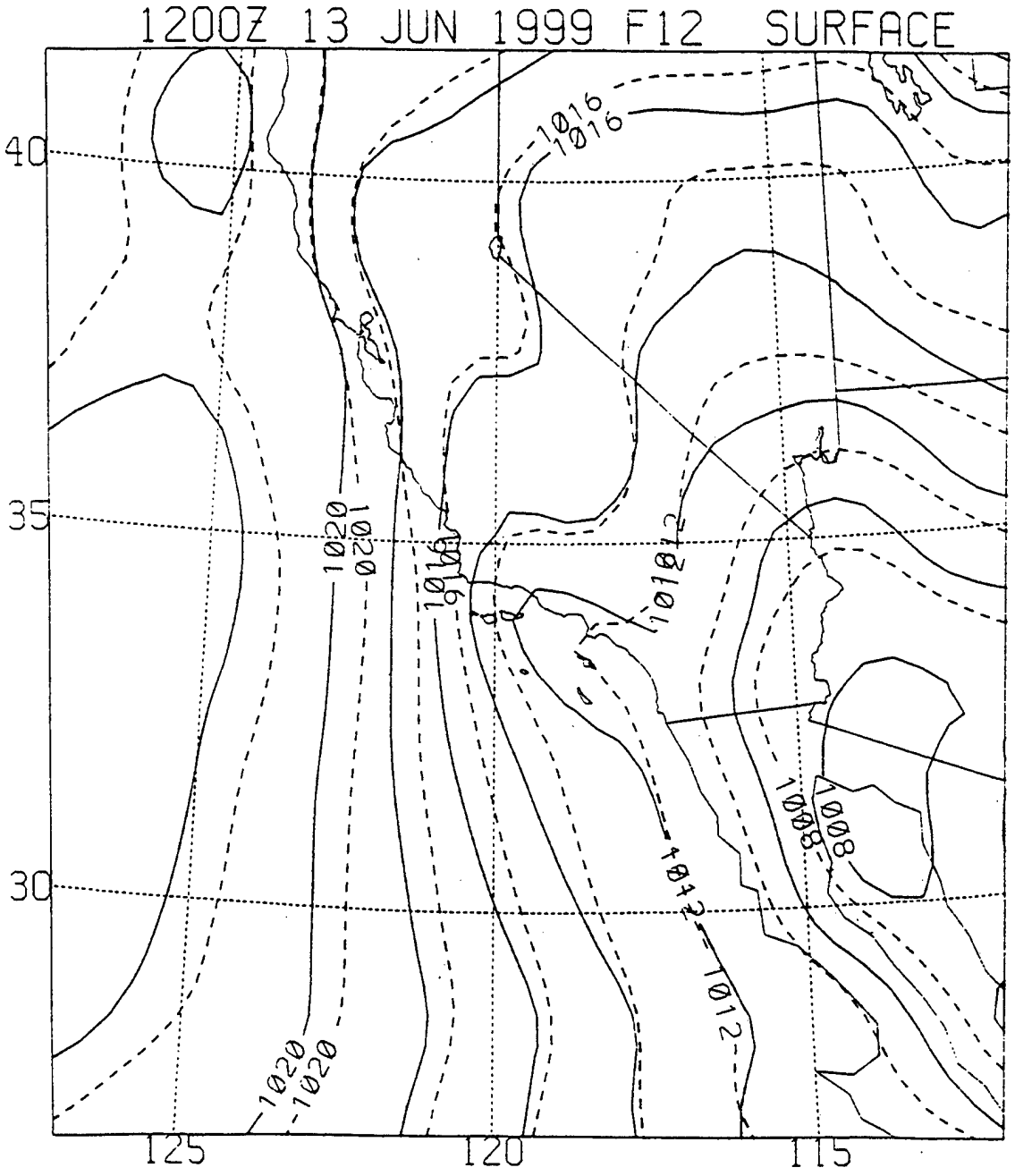

Figure 12. Outer nest (45 km) sea level pressure forecast for 13 June 12z f12 (12-hour forecast = solid line), and model analysis for 14 June 00z f00 (dashed line). Contour interval = 2 mb.

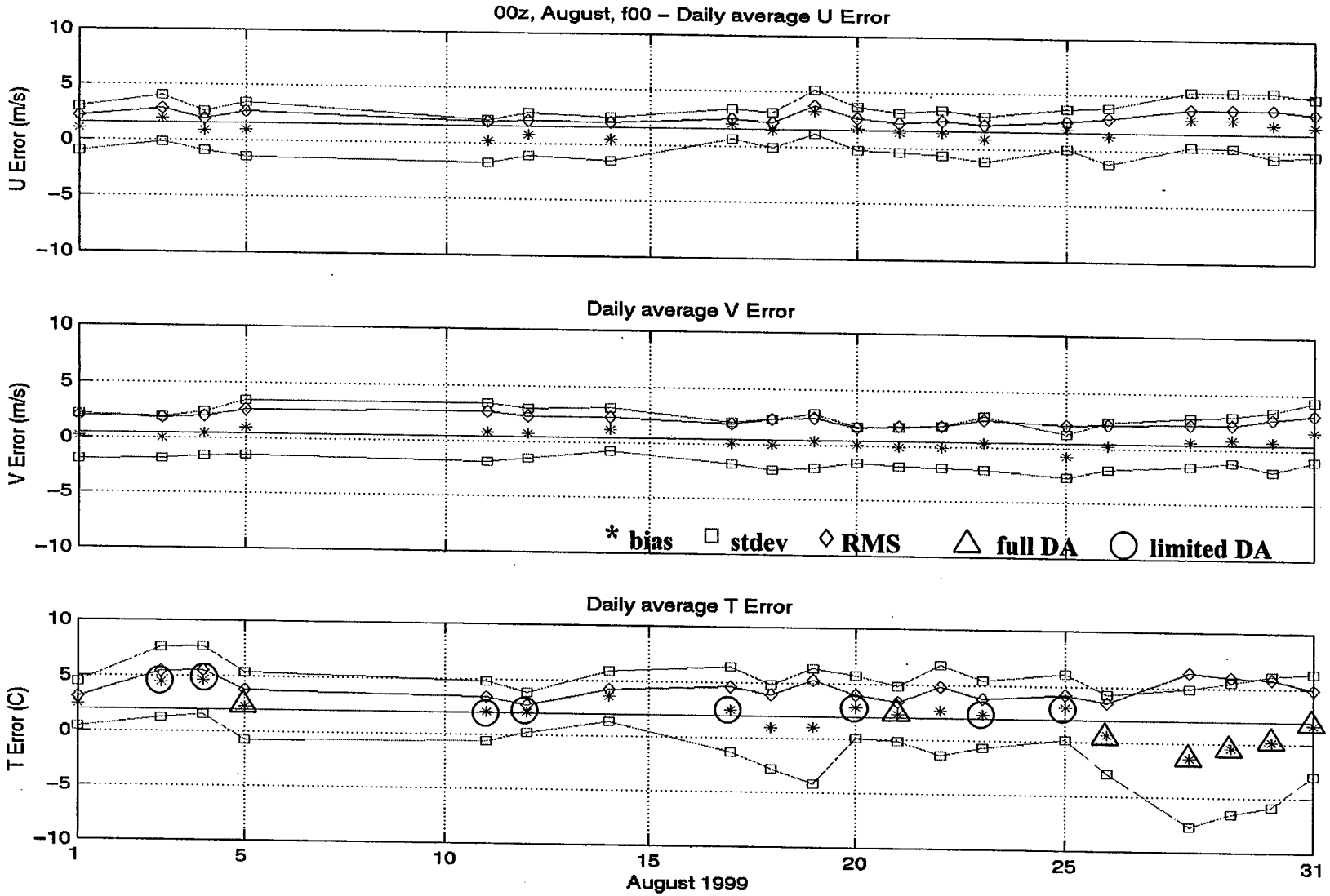

Figure 13a. August time series: 00z model run analysis (f00) with full and limited data assimilation (DA) highlighted.

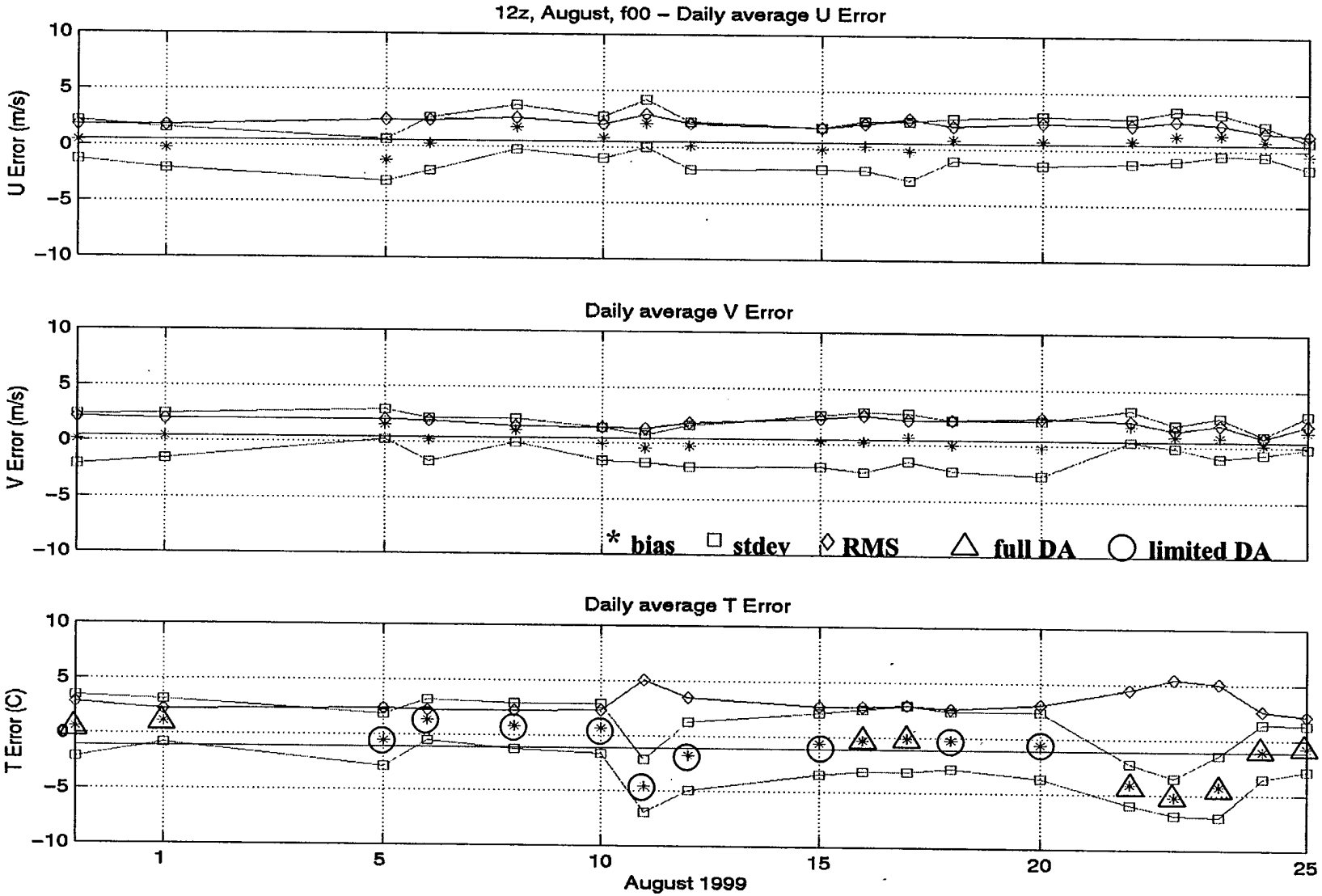

Figure 13b. August time series: 12z model run analysis (f00) with full and limited data assimilation (DA) highlighted.

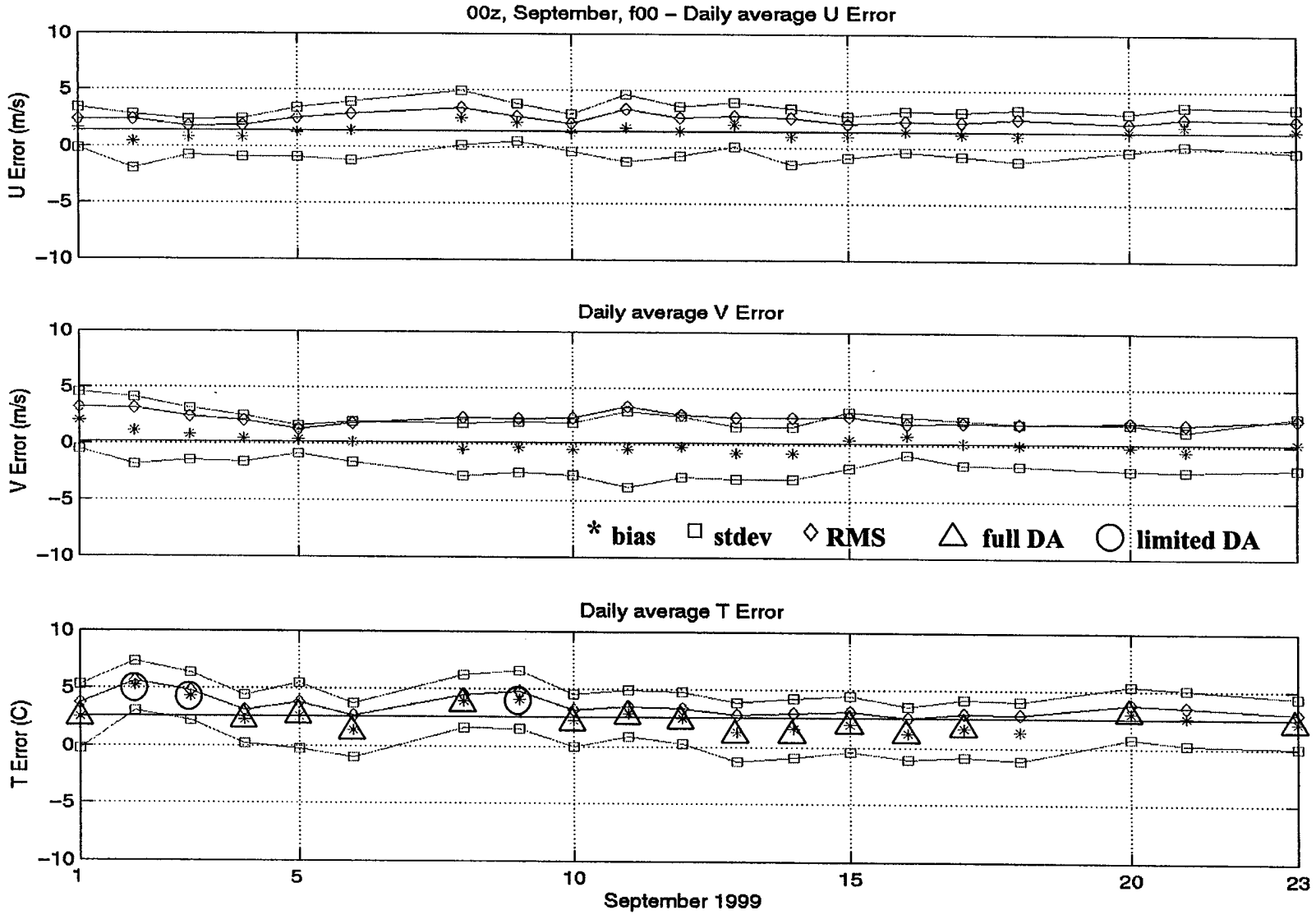

Figure 14a. September time series: 00z model run analysis (f00) with full and limited data assimilation (DA) highlighted.

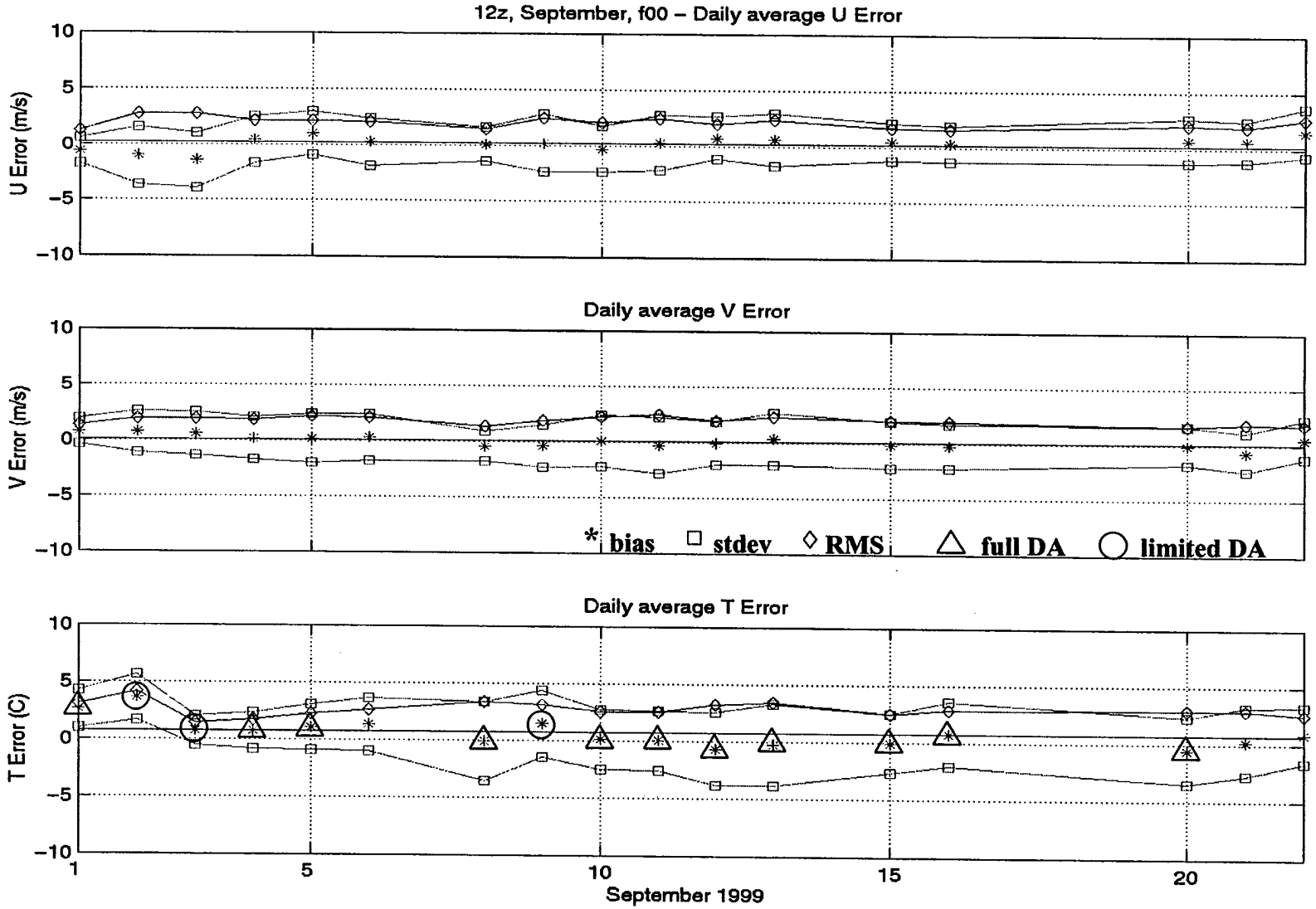

Figure 14b. September time series: 12z model run analysis (f00) with full and limited data assimilation (DA) highlighted.

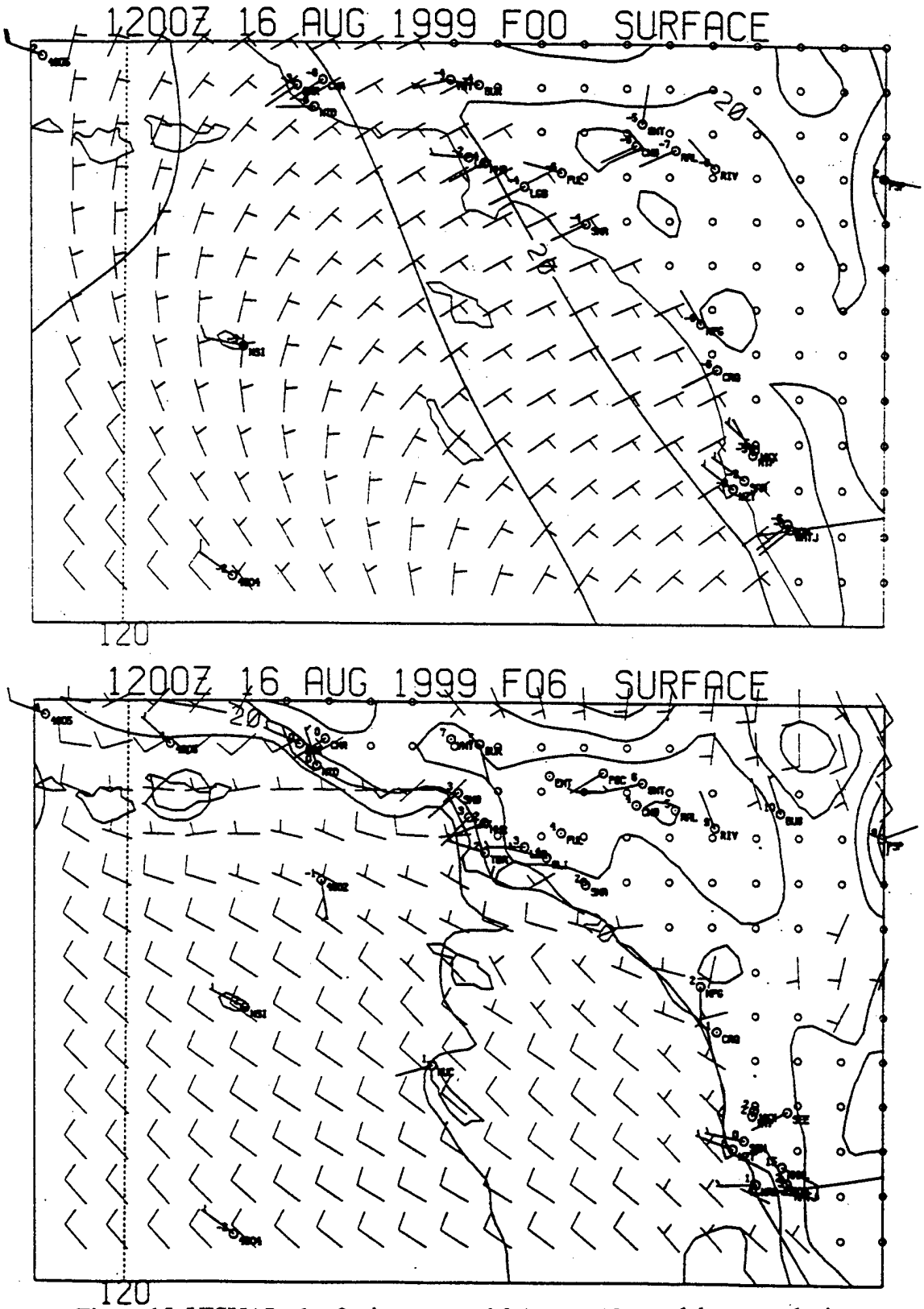

Figure 15. VISUAL plot for inner nest, 16 August 12z model run, analysis and 6-hour forecast (f00 and f06). Contour interval of 2 °C.

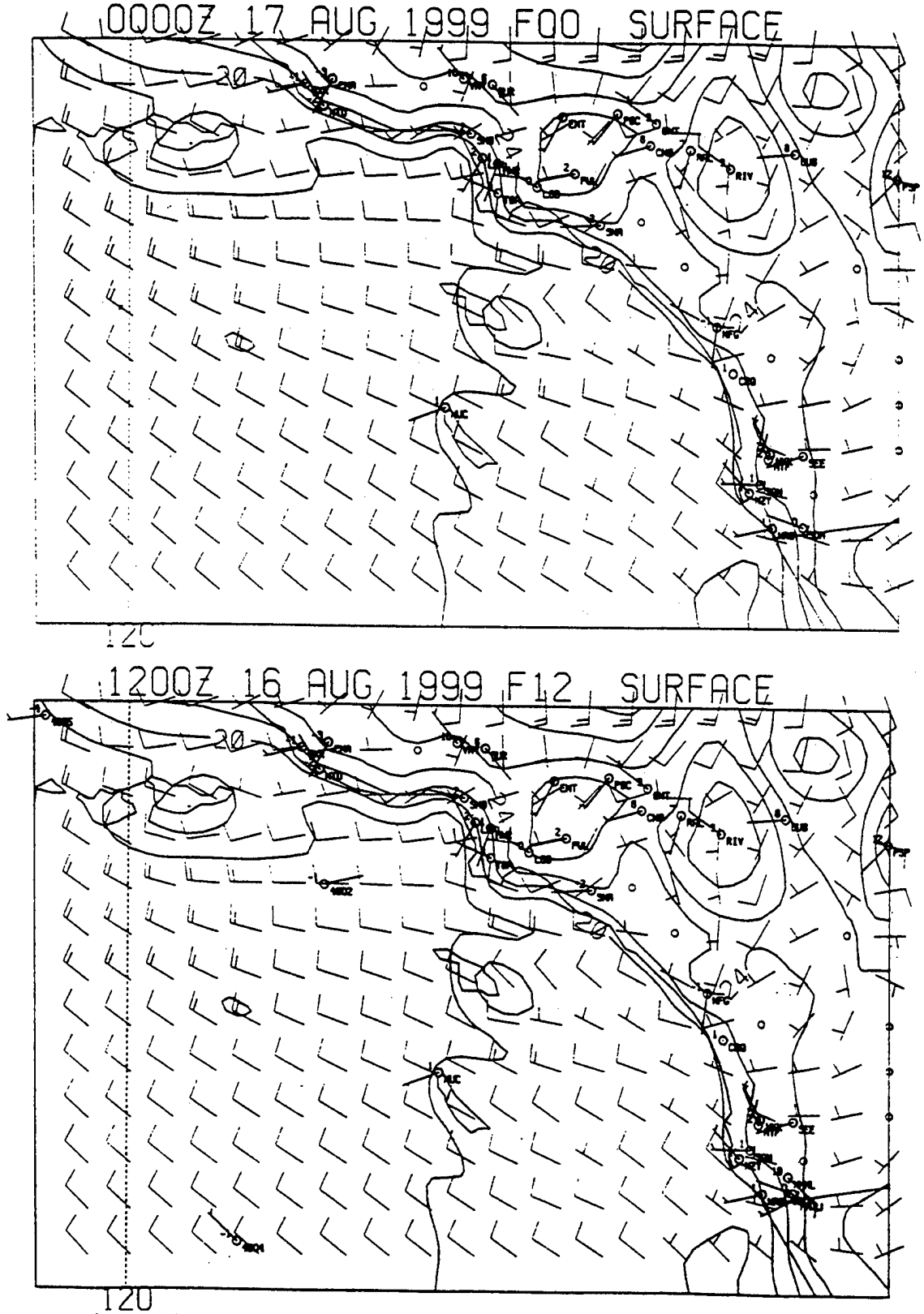

Figure 16. VISUAL plot for inner nest, 16 August 12z model run, 12-hour (f12) forecast and 17 August 00z model run analysis (f00). Contour interval of 2 °C.

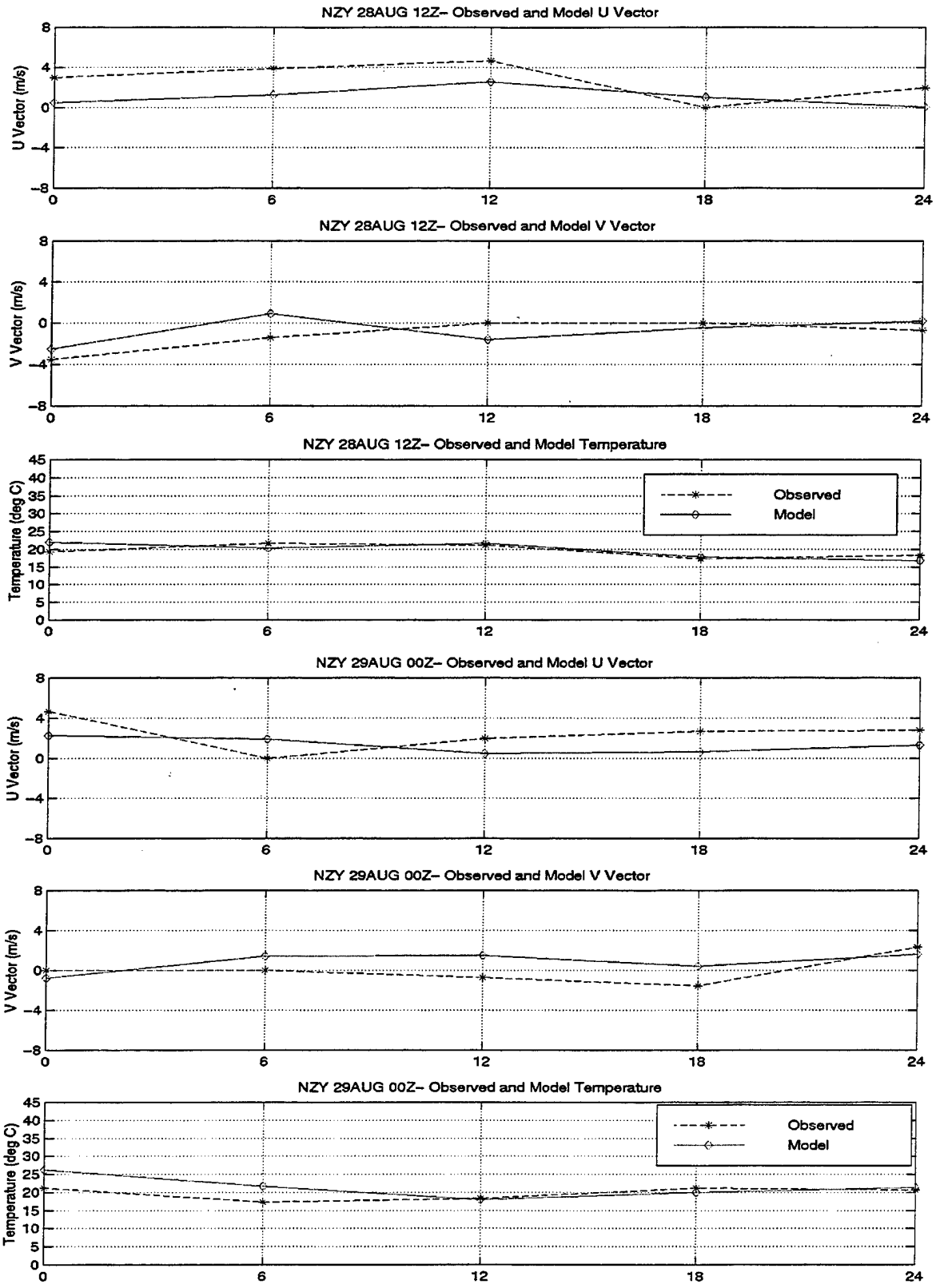

Figure 17a. North Island (NZY) time series for u, v, and T for 28/12z and 29/00z model runs.

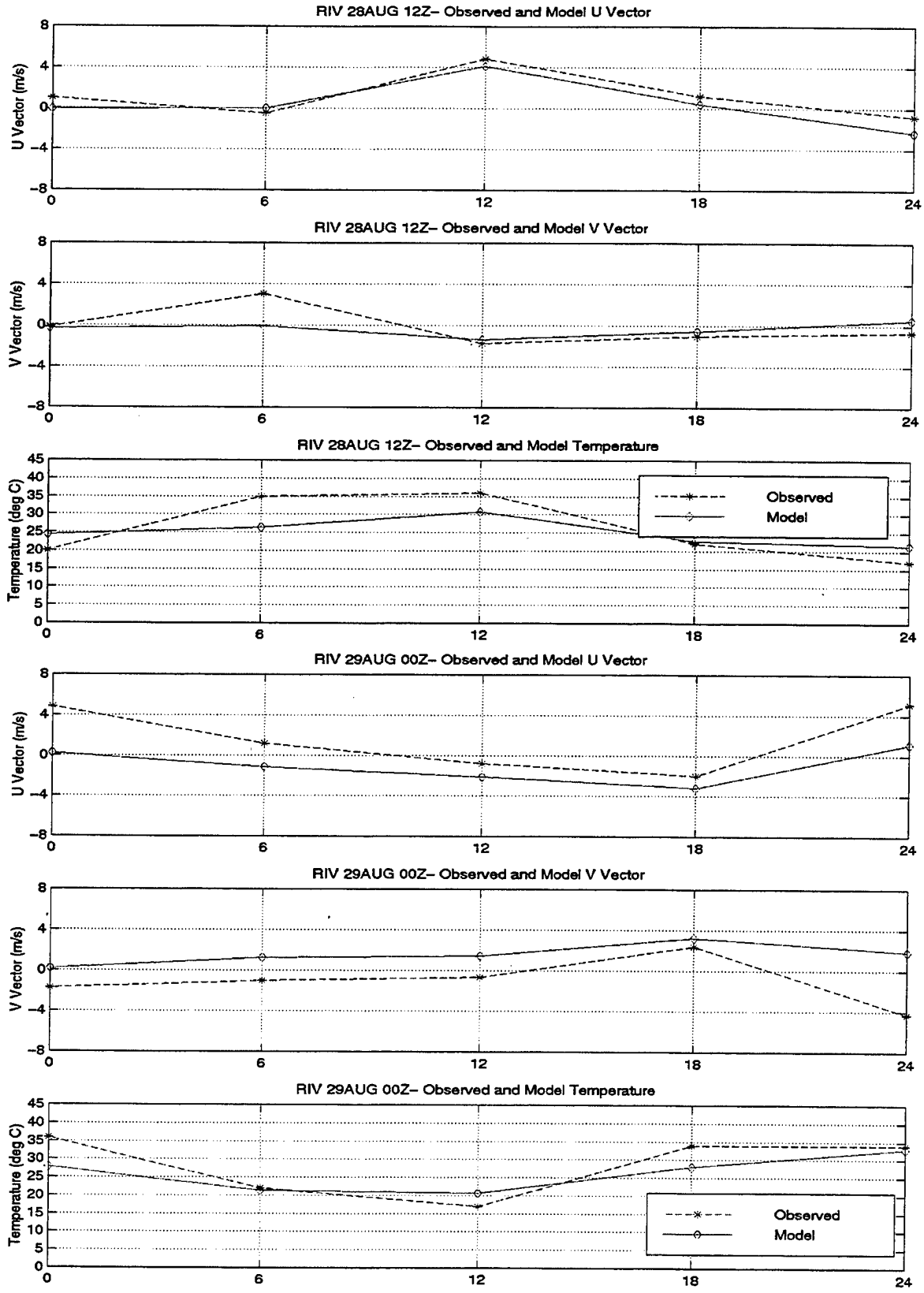

Figure 17b. Riverside (RIV) time series for u, v, and T for 28/12z and 29/00z model runs.

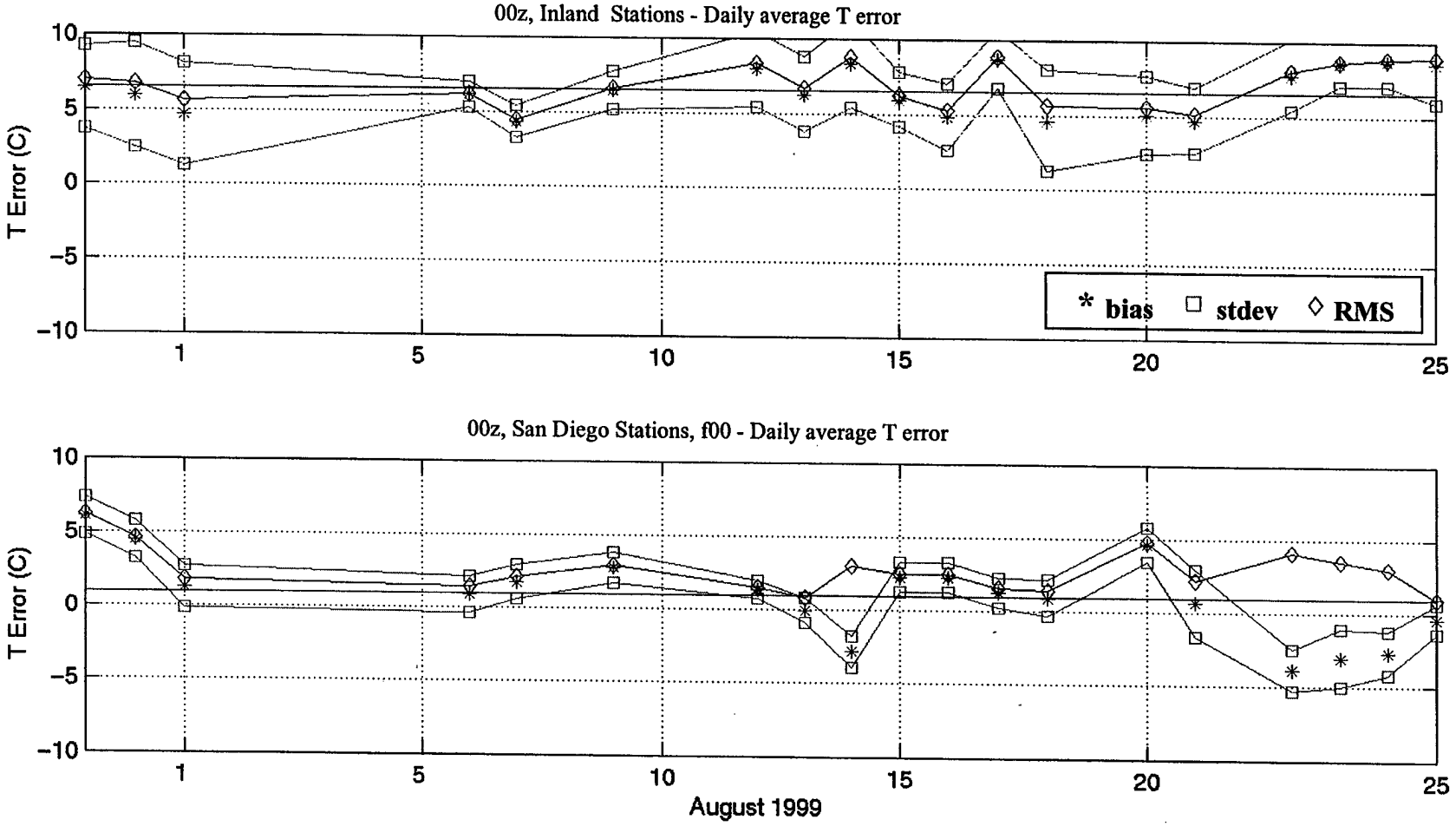

Figure 18. Temperature time series for Inland and San Diego Stations: 00z model run forecast.

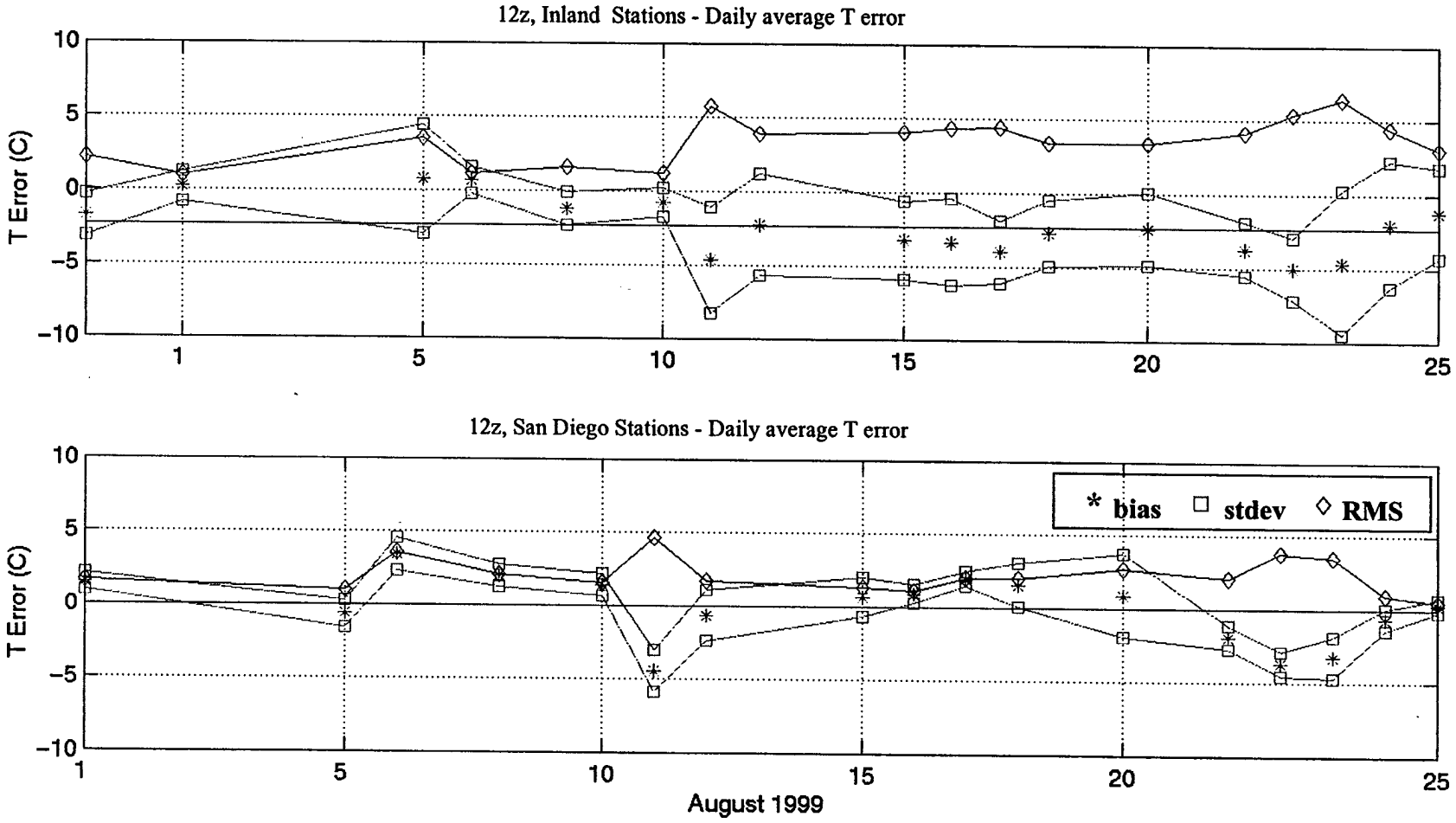

Figure 18b. Temperature time series for Inland and San Diego Stations: 12z model run forecast.

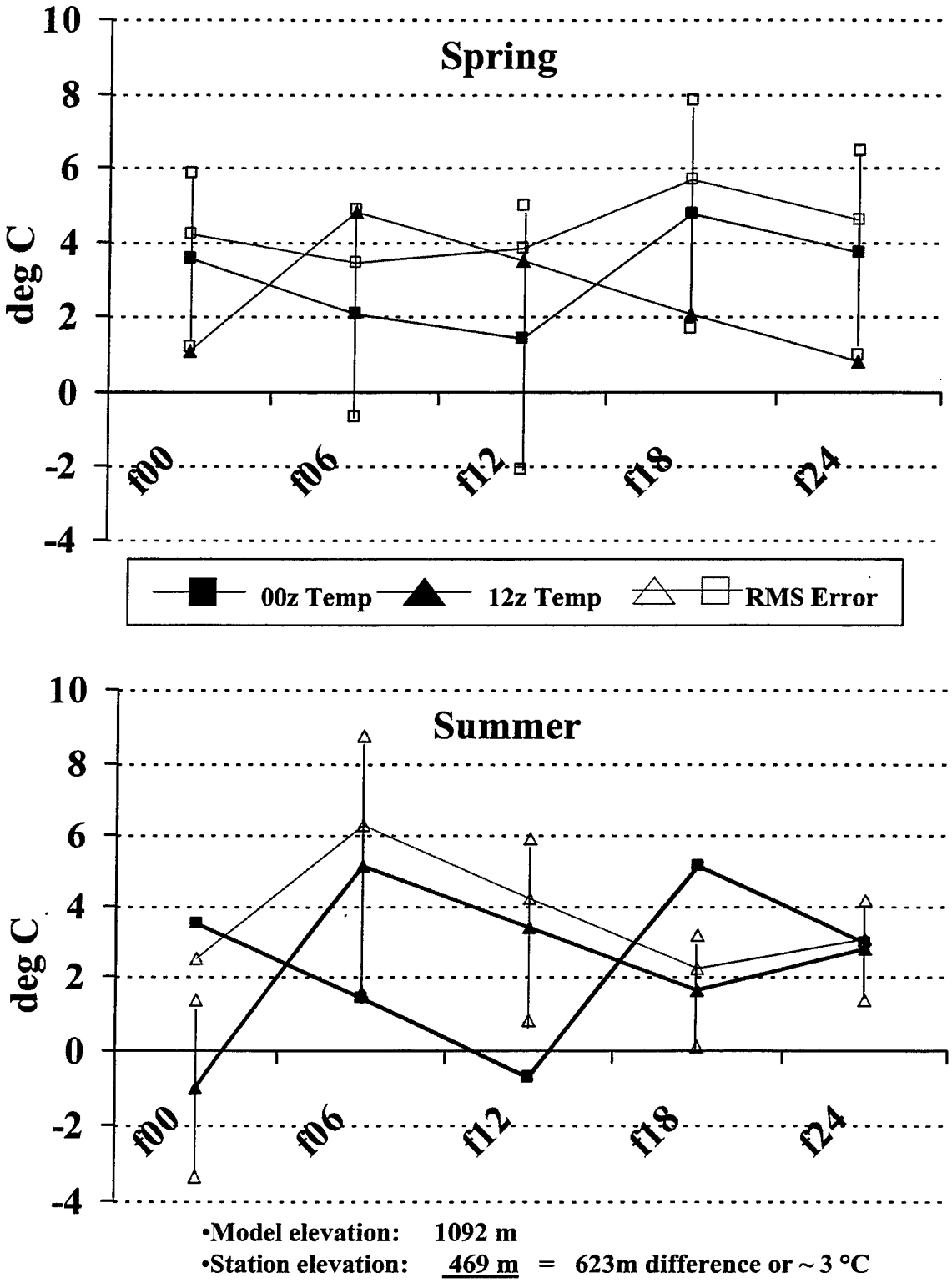

Figure 19. Riverside (RIV) temperature error growth for spring and summer.

LIST OF REFERENCES

Anthes, R.A. 1986: The General Question of Predictability. *Mesoscale Meteorology and Forecasting,* P.S. Ray (Ed.), Amer. Meteor. Soc., 636-655.

Anthes, R.A. and D.P. Baumhefner, 1984: A diagram depicting forecast skill and predictability. Bull. Amer. Meteor. Soc., 65, 701-703.

Cooperative Program for Operational Meteorology, Education and Training (COMET), 1998. Operated by Univ. of Colorado Atmospheric Res. and sponsored by the National Oceanic and Atmospheric Administration. [Available from COMET Program,: P.O. Box 3000, Boulder, CO 80307-3000; (phone) 303-497-8470; (fax) 303-497-8491.]

Doyle, J., 1997: The influence of mesoscale orography on a coastal jet and rainband. Mon. Wea. Rev., 125, 1465-1488.

Gunderson, C., 1999. Early returns on the San Diego local mesoscale modeling initiative. NPMOC San Diego, CA, 11 pp. [Available from Commanding Officer, NPMOC San Diego, PO BOX 357076, San Diego, CA, 92135-7076, Tel. (619) 545-6027.]

Hodur, R.M., 1997: The Naval Research Laboratory's Coupled Ocean/Atmosphere Mesoscale Prediction System (COAMPS). Mon. Wea. Rev., 125, 1414-1430.

Hovermale, J.B., 1986: Assimilation and initialization of atmospheric data into numerical prediction models. In: Mesoscale meteorology and forecasting, P.S. Ray, Ed., Am Meteor. Soc., 597-613.

Miller, D.K., 1999: Considerations in building and using a real-time mesoscale numerical forecast system. Class notes for *Forecasting analysis and prediction course.* Department of Meteorology, Naval Postgraduate School, 15 pp.

Naval Doctrine Command, Publication 1, Norfolk, VA, 1994: *Naval Doctrine Publication 1, Naval Warfare*, 74pp. [Available from Navy Publications and Forms Directorate, 5801 Tabor Ave, Philadelphia, PA, 19120-5099.]

Naval Pacific Meteorology and Oceanography Center (NPMOC) San Diego, CA, 1995: *Forecaster's Handbook for NAS North Island.* NPMOF San Diego,

CA, 124 pp. [Available from Commanding Officer, NPMOC San Diego, PO BOX 357076, San Diego, CA, 92135-7076, Tel. (619) 545-6027.]

Nuss, W.A., and D.W. Titley, 1994: Use of multiquadratic interpolation for meteorological objective analysis. Mon. Wea. Rev., 122, 1611-1631.

Naval Research Laboratory, cited 1999: TAMS/RT Homepage. [Available on-line from http://stratus.nrlmry.navy.mil/.]

Perkey, D.J., 1986: Formulation of mesoscale numerical models. In: Mesoscale meteorology and forecasting, P.S. Ray, Ed., Am Meteor. Soc., 573-596.

Reiss, A.J., 1999: Evaluation study of the Tactical Atmospheric Modeling System/Real-Time (TAMS/RT) at NPMOC San Diego. M.S thesis, Dept. of Meteorology, The Naval Postgraduate School, 90 pp. (submitted to NTIS). [Available from Department of Meteorology, Naval Postgraduate School, 589 Dyer Road, Room 254, Monterey, CA 93943-5114, Tel. (831) 656-2516.]

Sashegyi, K.D., and R.V. Madala, 1992: Initial conditions and boundary conditions. *Mesoscale Modeling of the Atmosphere,* R.A. Pielke and R.P. Pearce, Eds., Amer. Metero. Soc., 1-12.

Thompson, W.T., T. Haack, J.D. Doyle, S.D. Burk, 1997: A nonhydrostatic mesoscale simulation of the 10-11 June 1994 coastally trapped wind reversal. Mon. Wea. Rev., 125, 3211-3230.

Warner, T.T., 1992: Modeling of surface effects on the mesoscale. *Mesoscale Modeling of the Atmosphere,* R.A. Pielke and R.P. Pearce, Eds., Amer. Metero. Soc., 21-27.

INITIAL DISTRIBUTION LIST

No. Copies

1. Defense Technical Information Center.....2
   8725 John J. Kingman Road, STE 0944
   Ft. Belvoir, Virginia 22060-6218

2. Dudley Knox Library.....2
   Naval Postgraduate School
   411 Dyer Rd.
   Monterey, California 93943-5101

3. Chairman, Code MR/Wx.....1
   Department of Meteorology
   Naval Postgraduate School
   Monterey, California 93943-5101

4. Chairman, Code OC/Ga.....1
   Department of Oceanography
   Naval Postgraduate School
   Monterey, California 93943-5101

5. Professor Wendell A. Nuss, Code MR/Nu.....1
   Naval Postgraduate School
   Monterey, California 93943-5101

6. Commander.....1
   Naval Meteorology and Oceanography Command
   1020 Bach Boulevard
   Stennis Space Center, Mississippi 39529-5005

7. Commanding Officer.....1
   Naval Pacific Meteorology and Oceanography Center San Diego California
   P.O. Box 357076
   San Diego, CA 92135-7076

8. Commanding Officer.....1
   Fleet Numerical Meteorology and Oceanography Center
   7 Grace Hopper Ave., Stop A
   Monterey, CA 93943

9. Mr. John Cook, Code 7542.....1
   Naval Research Laboratory Monterey California
   7 Grace Hopper Ave., Stop 2
   Bldg. 702, Rm. 113
   Monterey, California 93943-5502

10. Dr. Ed Harrison.....1
    Space and Naval Warfare Systems Command (PMW-185)
    53560 Hull St.
    San Diego, CA 92152

11. LCDR Oscar E. Monterrosa.....5
41 Bai-Gorry Place
Walnut Creek, CA 94598